WATER EXCHANGE AND CHANNEL FRICTION RELATED TO TIDAL FLOW IN TUDOR CREEK SYSTEM,KENYA COAST,WETERN INDIAN OCEAN

Michael Mutua Nguli
Kenya Marine And Fisheries Research Institute.,
Mombasa., Kenya.

Thesis submitted for partial fulfilment of Masters of science Degree in physical oceanography, Department of Oceanography, University of Göteborg, SWEDEN,

May, 1994.

ABSTRACT

The Tudor creek system, located in mid-Kenya coast is formed by a sinuous channel,Tudor channel, between Mombasa port and Tudor harbour, which connects the inner wide and shallow basin,the Tudor creek, to Kilindini harbour and the Western Indian Ocean. Two seasonal rivers,Kombeni and Tsivu enter it. The creek is surrounded by mangrove wetlands,while it's off-shore area is shielded by shore-parallel reefs on both sides of the entrance. We have studied the tidal flow in the channel by RCMs and the tidal heights within the creek and outside with tide gauges obtaining the following results.The tide is semidiurnal with a form number of 0.18. The neap and spring tidal range is 1.7 m and 3.1 m in the creek. The flood tide lasts 6.5h while ebb tide extends for 6.3h. Mean flood and ebb currents are 0.36 ms^{-1} and 0.40 ms^{-1}respectively. There is a marginal phase lag between the entrance and the creek. A high evaporation compared to fresh-water input during peak dry period, influence the salinities. During this season the creek is well mixed with lower salinity water on the oceanic side and high salinity water in the creek. The average volume flux due to the tide is 2600m^3s^{-1} but the net exchange of water related to the residence time is 60 m^3s^{-1}. The residence time as determined from the NE monsoon peak dry season is of the order of two weeks.The bottom layer parameters; friction velocity, roughness length and drag coefficient have been estimated from pendelum current measurements assuming a logarithmic profile. Average values were 0.04 m s^{-1}, 0.34 m, and 8.3 x 10^{-3} respectively. Heat flux and radiation balance is studied on the basis of temperature measurements.

Keywords: **creek; evaporation; water exchange; advective and diffusive heat; residence time; drag coefficient; friction velocity; roughness length; dissipation;Tudor creek; Kenya coast.**

Abstract

Table of content

1.0 INTRODUCTION

Hydrodynamic characteristics of a coastal creek system is governed by local water balance, morphology, tidal and wind mixing. However, the residence of time of the creek is related to the distribution of salinity in the system and can be estimated once the salt gradient and the local water balance is known. The situation where salinity increases towards the ocean is the classical estuarine case. Such systems have received tremendous amounts of interest compared to the opposite situation where salinity decreases towards the ocean (e.g. Wolanski ,1989, Wolanski et.al., 1990 , Wolanski and Bunt, 1980). In the latter situation, evaporation exceeds freshwater input and such a system is described as an `inverse estuary´. 'Inverse estuaries' are typical for a large number of creek systems in equatorial coastal regions. One such system, the Tudor creek system, is considered in this thesis.

The Tudor creek is located on the mid-Kenyan coast . It has a surface area of 22 km^2, and almost surrounded by mangrove wetland. The creek can be described as slightly choked where friction in it's single 4km long, 20m deep inlet is may be important (Wolanski,1990).

There is little ~~existing~~ information on hydrological and hydrodynamic characteristics of this system, despite the persistent questions posed by and biological scientists currently involved in nutrient and plankton dynamics regarding mixing, and residence times for the system. In an attempt to answer their questions a series of oceanographic measurements were carried out in the creek and it's channel areas between June 1992 and February 1994.

This thesis is an effort to use temperature and salinity measurements,tide gauge data, and current measurements ~~to study~~ the water exchange in Tudor creek system.That is (1) determine residence time for the peak dry season during the North East monsoon period, (2) use harmonic and spectral analysis in order to examine the tidal constituents and their importance,(3) determine volume fluxes including residence time and the net heat flux through the channel and (4) investigate the bottom layer parameters in the

channel.

2.0 THE STUDY AREA

2.1 Bathymetry

Tudor creek system is formed by a sinuous 400-500 m wide,10-20 m deep and 4 km long channel,Tudor channel, which occur between Mombasa Port and Tudor harbour, and an inner wide basin with a depth of 3-5 m at MSL (fig. 1). The channel connects to Kilindini harbour south of Mombasa Island and to the western Indian Ocean. Two seasonal rivers ,Kombeni and Tsivu enter the system. The shore line is surrounded by mangrove wetlands. Mudflats also occur in the fringes of the mangroves. The volume of the channel is $20x10^6$ m^3 and that of the creek $60x10^6$ m^3 at MSL. The area of the creek is $20x10^6 m^2$.

2.1 Hydrological and meteorological characteristics

The climate of the area is tropical, with four characteristic monsoon periods . Two of the stages ,the North East (NE) monsoon and the South East (SE) monsoon are the main ones while the others are transitional. NE monsoon stage occur from November to March , with northeasterly winds blowing at an average speed of 8 ms^{-1}, while the SE monsoon is from mid-April to October with southerly winds and average speed of 9.5 ms^{-1}. The transitional stages occur in late October and mid-April (Jonson et . al 1982, Griffin, 1972). The SE monsoon period is more markedly influenced by land-sea breeze than the NE monsoon period.

Two dry and two rainy seasons are closely linked to the monsoon stages. SE monsoon `peak dry season´(PDS) lasts from June to early October and the NE PDS from

November to the end of March. Peak short rain season (PSRS) is from November to December, while the `peak long rain season´ (PLRS) is from April to June.

Rainfall ranges from 762 to 1270mm $year^{-1}$ for the coastal area. The range during 1992-93 was 600-1000mm $year^{-1}$ with about 40% falling during the PLRS and 30% in PSRS (fig2.1(i)). The annual mean temperature is 25.4^{o}C. The lowest values, 24^{o}C occur in August while the highest values ,28-29^{o}C occur in February-March. Relative humidity averages 80%, but range from 92-94% during the night and early morning and drops to 60-70% in the afternoon . The potential eveporation rates from pan measurement ranges from 2200 to 2400 mm $year^{-1}$(Griffin,1972). The mean discharge from Kombeni and Tsivu rives is less than 1 m^3s^{-1} (Norconsult ,1975) but varies with season. Mean ~~spring tide~~ as determined from the tide gauge in Mombasa is of the order of 3 m (Pugh, 1979).

3.0 METHODS AND MATERIALS

3.1 Sea level and current measurements with tide gauges and RCMs.Hydrographic surveys

Field measurements on tidal elevation, currents ,salinities and temperatures were made by using Micro-Tide pressure gauges,RCMs of type Sensordata SD6000, pendelum current meters (see 3.2;Haamer,1974) and an Aanderaa in situ salinometer.

Meteorological data consisting of air temperature,wind speed,rainfall,evaporation, temperature and relative humidity were obtained from Moi International Airport , 4 km from the study area. The study area and the positions of the instruments are shown in fig.1. One tide gauge was located at the ocean side of Tudor channel whereas an other tide gauge was located inside the channel.The current meters, RCM93 and RCM94, were deployed 10m above the bottom in two slightly different mid-channel positions off Ras Kindomoni (stn #6), where the depth of the channel is approximately 20m. Two cross-sections ,one at station #6 and the other at station #5 were used for salinity, temperature and pendelum current measurements.

Salinity and temperature measurements were made twice per month from July 1992 to May 1993 11/2 hour before high or low water during spring and neap periods all along the Tudor creek (#1-#7). Pendulum current measurements were also made twice a month for three months. Data from the tide gauges and RCM94,with sampling interval of 2 min. and 5 min. respectively exist simultaneously from 4th to 22nd February 1994, whereas RCM93 , with sampling interval of 10 min, was deployed between 12th January and 2nd February 1993. The period of measurement for RCM93 corresponds to that of the salinity, temperature and pendelum current measurements and are treated together. Unlike the RCMs current meters which record and store data internally the pendelum current meters require special attention. They are briefly described below.

3.2 Pendelum current measurements.Technical descriptions

Each meter consists of a one point suspeded fin ,whose edge is directed against the current. The fin is inclined at different angle to the vertical depending on the current velocity. A registration device consisting of cylindrical plexiglass box filled with melted gelatine solution that solidifies at about $30^{o}C$ (depending on the solution) is mounted on the fin. A compass needle (the pendelum) is freely hanging in the box showing the angle of the fin in relation to the north pole of the compass. Before measurments are started, the box is heated and the gelatine melts so that the compass needle is freely suspended, when the fins are lowered into the water, the gelatine solidifies, thereby locking the compass needle in a position depending on the strength and direction of the current. To measure the vertical current profile pendelums three stations,approximately 180 m apart, were selected along the transect at station # 6 . The pendelum current measurements were made twice a month one and a half an hour before flood or ebb periods respectively. A total of 14 pendelums were used. The two side stations each consisted of three pendelums hooked on a vertical line every 1 to 3 meters whereas the middle station consisted of 9 pendulums similary hooked except for the lowest 4 pendulums with 1 meter spacing from the sea-bed and from each other (see mooring fig.2). After 30 minutes,they were surfaced and the angle of inclination recorded, then the angles were used to read off the current velocity from a calibrated curve.

3.3 Analysis of time series of tide and current meter measurements

The tide and current meter measurements were subjected to harmonic and spectral analysis (see below). The recordings from the tide gauges however were cut off during the HWS due to the limited instrument ranges compared to the maximum tidal range. Therefore sea levels near HWS were calculated by using a Matlab spline function. Fig 3a shows the original data,while fig.3b shows the time series plots including the

calculated HWS values and fig3c. After this procedure the harmonic analysis program was used on the time series from both the tide gauge stations; the creek station and the one on the oceanic side . Table 3-5 shows the result for six main constituents.

Before doing harmonic analysis on the RCM data from stn 6, the main direction for the RCMs were determined from stick plots shown in fig.4 a-b. and fig.4c. This direction was set to 350^{o} from which the length and cross-channel velocities were calculated according to:

$$u = U\cos(350-\theta)$$

$$v=U\sin(350-\theta)$$

where U is the measured velocity and θ is the measured direction, u is the along channel component and v the cross-channel component. u is plotted for RCM93 and RCM94 (stn 6) in fig. 5a-b. Harmonic analysis was made on the length components fig.5a-b.

The pendelum data were similarily decomposed into u and v components and the length component, u was used for calculation of volume transport at occasions when pendelum cross-sections were taken. In addition the pendelum measurements were used for determination of bottom friction parameters in the channel.

3.4 Theory on harmonic analysis

Tides are caused by gravitational influence of celestial bodies on each other. Gravitational influence on the earth is mainly due to the moon and the sun. The tide generating forces due to the moon are greater than those cause by the sun. Tides are usually divided into species, that is long -period diurnal and semi-diurnal. Long-period tides have periods ranging from 14 days to upwards. Period for diurnal and semi-diurnal tides are roughly one 1 and 1 1/2 days respectively. Periods of less than a day are caused by meteorological or friction forcing. Tidal species are further divided into constituents which are known precisely from astronomical observations (Neuman and Pierson ,1966). Table 1., gives a list of some of the tidal constituents which has been used in the study, included also are six of the shallow water tides which tend to resonate in coastal embayments.

Features of any tide regime are primarily determined by two semi-diurnal and two diurnal constituents namely M2, S2 and K1, O1 respectively.

The form number (F) defined as the ratio of the sum of the amplitudes of the diurnal components (K1+O1) to the sum of the amplitudes of the semi-diurnal components (M2+S2), that is

$$F = (K1+O1) / (M2 + S2)$$

The criteria for classification based on the form number is given by table 2. The amplitude can be determined from harmonic analysis.

Time series data may be written as the sum of a finite number of COSINE (or SINE) waves. This is because in practice, the infinite sum of SINE and COSINE terms which satisfy the Dirichlet conditions i.e, (1) finite number of discontinuities in one period (2) finite number of maxima and minima in one period and (3) the integration over a period to yield finite value,which reduces to sum of the fundamental period. With digital processing of data this is possible because any component having a frequency higher

than 1/2 dt (where dt is the sampling interval) cannot be resolved,because to represent a periodic function at least three points are necessary. This cut -off frequency is known as the Nyquist frequency. The following is the harmonic series expression for k tidal constituents,

$$H(t) = \sum a_k \sin(\omega_k t) + \sum_k a_k \cos(\omega_k t)$$

where ω_K and a_K represents the characteristic frequency and amplitude of the k^{th} constituent.

Least square method requires that,

$$\sum_{n=0}^{N} (H_n - H(t_n))^2 = \text{minimum} \quad ,$$

This requirement is satisfied by

$$\frac{\partial M}{\partial a} = 0 \text{ and } \frac{\partial M}{\partial b} = 0$$

where

$$\frac{\partial M}{\partial a} = -2 \sum_{n=0}^{N} \cos\omega t_n (H_n - a\cos(\omega t_n) - b\sin(\omega t_n)) = 0 \quad ,$$

$$\frac{\partial M}{\partial b} = -2 \sum_{n=0}^{N} \sin\omega t_n (H_n - a\cos(\omega t_n) - b\sin(\omega t_n)) = 0 \quad ,$$

The above equations simplify to

$$\sum_{n=0}^{N} H_n \cos(\omega t_n) = \sum_{n=1}^{N} (\cos^2(\omega t_n)) + b \sum_{n=1}^{N} (\sin(\omega t_n)\cos(\omega t_n))$$

$$\sum_{n=0}^{N} H_n \sin(\omega t_n) = \sum_{n=1}^{N} (\sin(\omega t_n)\cos(\omega t_n)) + b \sum_{n=1}^{N} (\sin^2(\omega t_n))$$

$$A_1 = \sum_{n=1}^{N} (\cos^2(\omega t_n)) \quad B_1 = \sum_{n=1}^{N} (\sin(\omega t_n)\cos(\omega t_n)), \quad C_1 = \sum_{n=0}^{N} H_n \cos(\omega t_n),$$

$$A_2 = \sum_{n=1}^{N} (\sin(\omega t_n)\cos(\omega t_n)), \quad B_2 = \sum_{n=1}^{N} (\sin^2(\omega t_n)), \quad C_2 = \sum_{n=0}^{N} H_n \sin(\omega t_n),$$

$$a = \frac{C_1 B_2 - C_2 B_1}{A_1 B_2 - A_2 B_1} \qquad b = \frac{C_1 A_2 - C_2 A_1}{A_2 B_1 - A_1 B_2},$$

$$\text{Amplitude} = \sqrt{a^2 - b^2},$$

4.0 RESULTS AND DISCUSSION

4.1 Tides and tidal currents

4.1.1 Comments on harmonic analysis of tide and current meter measurements

The harmonic analysis equations were solved using a Matlab program (Cederlöf, 1993) The results are presented in table 3-5 together with those of Pugh,1979 who studied the tide in Kilindini harbour on the opposite side of Mombasa island using the Admirality tide gauge. Our time series, however are too short to obtain reliable results for many components (we used seven in all). This is particulary true for the phases.

The results however show that the tide is semi-diurnal with most of the energy concentrated in M_2. The form number is 0.18. The amplitude for the M_2 closely agree with the value obtained by Pugh,1979. The problem with different phase lags is discussed by Odido, 1994.

The mean spring tidal range is 2.76 m at the entrance and 3.12 m in the creek (comp.Norconsult, 1975). The difference, however is probably not significant (see also table.7 for hydrographic characteristics of Tudor creek). We experienced some problems with the instrument calibrations, which including the already mentioned 'cut offs ' at HWS make the details uncertain. It is not reasonable to draw any direct conclusion, especially as we would rather expect a decrease in the range inside the channel. Energy spectra (figs.5a-b) reveal the dominance of the M_2 tide thus establishing that the tidal currents in the creek are predominantly tidal. The residual currents show maximum value of $0.15ms^{-1}$inside the creek and $0.1ms^{-1}$ at the entrance. Slight fluctuation occur in the creek (fig.6a).

The data from the recording current meters, deployed in the channel, were also analysed with the help of harmonics analysis (and spectral analysis) so as to compare with the results obtained from tidal data (table 3).This was done exclusively for the larger components. The results are shown in tables 4 and 5.

4.1.2 Current measurements

The RCMs gave a mean current velocity (u) of 0.37 m s^{-1} with a maximum velocity range of 0.60-0.70 ms^{-1} (fig 4c-d). The pendelum current mesurements corroborated the results from the RCMs indicating mean flood velocities of 0.395 m s^{-1} in the direction of 350^{o},and maximum range of 0.40-0.60 m s^{-1}.

Alternatively, the velocity structure in the channel may be determined from the tidal elevations (Svedrup et al,. 1942 ,Defant,1961) as follows: Taking the surface area A_c of Tudor creek at MSL as $20x10^6$ m^2 and the cross-section area A_{xs} at stn #6 as 7832 m^2

and observed mean spring tide range H_c equal to 3 m, the total volume of water that flows into the creek in the time interval between low and high water is $A_c \times H_c$ m^3. The mean inflow, may be expressed as

$A_{xs}U_{av}.T/2,$

where U_{av}. is the average velocity during the half tidal period T/2 in which the flow takes place. The maximum velocity during that time is

$\pi/2 \times U_{av}.ms^{-1}$,

but the flow is not uniform through the cross-section. The mid-channel velocity may be 1/3 larger than the average and can be approximated from the expression

$$U_{max} = \frac{4}{3}\frac{\pi}{T}\frac{A_c}{A_{xs}}H_c$$

where U_{max} is the maximum velocity. The average current U_{av} is given by

$$U_{av} = \frac{A_c}{A_{xs}}\frac{H_c}{T/2},$$

When appropriate values are inserted in the expressions the average current is found to be 36 cms^{-1} with a maximum mid-channel velocity of 67 cms^{-1}. The values indicate a close agreement with those obtained from the pendulums and the RCMs.

The total horizontal displacement during one half tidal period when water flows in the same direction can be calculated from the expression

$L_d = U_{max}\int_0^{\pi}\cos \sigma t dt$

$$= 2\, U_{max} \frac{1}{\sigma}$$

$$= U_{max} \frac{T}{\pi}$$

If a value of 0.67 ms^{-1} is taken for U_{max}, then the total displacement is approximately 9.5km during a flood period, which is twice the length of Tudor channel. The result indicate that only 50% of the channel flow during flood reaches the creek area. By extracting a few tidal periods from the RCM data (fig.7a-b) we can see that although there is no asymmetry in the tide itself the current in the creek experience a considerable asymmetry with a rapid change from maximum flood velocities and to maximum ebb velocities the a slow change in the other way round. The reason for that feature could not be explained so far and but for different phase lags it is similar to Wolanski's (1989) features based on modelling of tide in Tudor (fig 7c).

4.1.3 Volume flux

The volume flux in the channel was estimated by multiplying the cross-section area (obtained by subdividing the cross-section at stn #6 into small squares, rectangles, and triangles using a navigation chart for the harbour) with the pendelums velocity (u) along the channel. Figure 8a shows the hypsographic curve for Tudor creek indicating the amount of water contained within the tidal area as a function of water level and figure 8b volume flux through the channel. The mean volume flux during flood is 2500 $m^3s^{-1}$and during ebb 2700 m^3s^{-1} . There is a small difference in the mean flux which could be caused by many different effects (the stick plot data (fig 4a-b) indicate that 350^o as main direction would underestimate slightly the inflow). The volume flux can be calculated also from the mean tidal range (3 m) and the area of the creek. For T=12.42hrs the mean flux is then 2650m^3s^{-1}.

4.2 Water Exchange

The average time a parcel spends in the inner part of Tudor creek is the residence time. The residence time is determined in relation to the ocean water. The residence time can be estimated from the salinity gradient and the sum of evaporation,precipitation and fresh water supply. It can also be estimated from tidal volume flux which assumes that one can calculate the mixing caused by the tidal plume occuring inside of the channel.
Since the salinity gradient vary with season (i.e depending on whether it is wet season or dry season), the residence time may to some extent depend on season.
In this section an attempt is made to estimate the residence time during the peak dry-season which occur from mid-June to October and from January to March (Griffiths, 1972) in the SE monsoon and NE monsoon respectively.

4.2.1 Salinity and temperature

The seasonal temperature and salinity variations from Kombeni river (stn #1) to the oceanic site (stn #7) are shown in fig.9. The figures indicate a steady increase of temperature and salinity values from the beginning of the two peak dry seasons. A summary over the various seasons is found in table 6.

The values are shown for peak dry period in 1992 (September to November) and peak dry period in 1993 (February-April). Results during peak short rain season 1992 and peak long rain season 1993, include only surface salinities which are not quite representative. However it is worthwile noting that there is a difference of 2.4 PSU at Kombeni river (stn #1) between peak dry season and peak rain season.
In the channel, near the entrance the mean salinity and mean temperature (averaged vertically and horizontally (stns # 5 and 6) for SE monsoon 35.19 PSU ,27.24^{o}C.

The salinity was slightly higher than during the NE monsoon (34.68 PSU ,27.80^{o}C)

Data from the creek (stns #2 to 4) indicated high salinities for both NE monsoon and SE monsoon peak dry seasons. Maximum salinities and temperatures in the creek occurred during the NE monsoon with mean values of 35.60 PSU,30.2^{o}; higher than those found in SE monsoon (35.49 PSU 27.6^{o}C). This shows an increase of the salinity of nearly 1PSU in the creek during the NE monsoon. From table 6. the temperature difference from the creek and the ocean' side is 0.66^{o}C for SE peak dry season. However for NE peak dry season this value is 1.56^{o}C, indicating increasing solar radiation during this period. The monsoon coincides with relatively clear skies and probably, lower latent heat flux due to a lower mean wind speed compared to the SE monsoon period. Daily variations in temperature were obtained from the tide gauges and are shown if figure10a-b, The values range from 24.8-32.2^{o}C in the creek, and 24.4-29.8^{o}C at ocean side. There is a slight difference between the temperature values obtained using salinometer (table 6) and those of the tide gauge. The difference may appear due to different reasons.

4.2.3 Salt balance equation-excess evaporation situation

From fig.9 and table 6, it is obvious that the salinity decreases from the creek towards the ocean for the dry period. It seems reasonable that this gradient is caused by evaporation which exceeds freshwater supply and precipitation during the dry period. The large mangrove swamps that fringe the creek and the large areas of tidal mud flats enhance evaporation. The mangroves do this by evapotranspiration, the mud flats through increased temperatures when exposed during low water periods (Wolanski, 1985). Here we shall try to determine the water exchange by making use of the observed salinity gradient during the PDS. First we give some theory.

Assuming a salinity in the creek (with volume V) of S_1 and in the ocean of S_o the salt balance is established according to :

$$\frac{d}{dt}(VS_1) = Q_o S_o - Q_1 S_1 \quad , \qquad 4.2.5a$$

or in steady state

$$QoSo = Q_1 S_1 \qquad 4.2.5b$$

Here, Q_o is the mean flow into the creek, and Q_1 is the mean out flow, see sketch of the flow in fig.11.

A volume balance is established according to:

$$Q_1 = Q_o - Q_e \, , \qquad 4.2.5c$$

where Qe is the net evaporation

By inserting equation 4.2.5c into 4.2.5b ,we obtain

$$Q_o = Q_e S_1 / S_1 - S_o \, . \qquad 4.2.5d$$

The residence time is defined as $T = V/Q_{max}$ where Q_{max} is the maximum of Q_1 and Q_o. To determine T and Q_o however we need an estimate of the net evaporation (see below)

4.2.4 Estimation of residence times from salinity measurements.

The pan evaporation in Mombasa amounts to 2300 mm per year, which implies a mean evaporation of 6.3mm per day for the Tudor creek. During the peak dry season it is reasonable to assume that both fresh water supply and precipitation are zero. Excluding evapotranspiration, the net evaporation Q_e is 1.5 m^3s^{-1}.

From equation 4.2.5d we then obtain (with S_1-S_0 = 0. 92), Q_0= 62 m^3s^{-1},and Q_1=60.5 m^3s^{-1}. Residence time = V/Q_0=15 days. As however Q_e may be larger during this peroid due both to evaporation and drought, it is possible that T is overestimated to some extent.

Wolanski (1985) has used an alternative salt balance equation (but principally similar) for a creek system which can be written as,

$$E_t S_{in} A_c = K A_{xs} \frac{dS}{dX}$$

where E_t = Evaporation

K = the longitudinal eddy dispersion coefficient,

A_{xs}= the average crossection area,

A_c = the horizontal area of the creek,

dS/dX= the salinity gradient.

Sin=salinity outside the creek

Tthe values for Tudor are, Et=0.6 x 10^{-2} m day^{-1}, S=35.60 PSU , A_c=20 x10^6 m^2 ,

A_{xs}=7800m^2

dS/dx = 0.92/8000

where δS is 0.92 from table 6. When these values are put in the above equation, the value of the eddy dispersion coefficient (K) is found to be 54 m $^2s^{-1}$.

4.3 Heat Exchange

4.3.1 Radiation balance

Flood usually implies that colder oceanic water is brought into the Tudor creek system while the ebb removes mixed creek water containing excess heat. Since the water exchange and the temperatures of the different waters have been measured (both within the hydrographic survey program and through tide gauge measurements), it is principally possible to calculate heat flux through the channel. We shall also establish a heat budget for the area.

The average heat flux through the Tudor channel per unit surface area is given by

$$Q_T = (Q_{sr} - Q_{lrbr} - Q_{ehl}) - Q_{rsr} - Q_{hcf}$$

where,

Q_{sr} is the solar radiation input,

Q_{rsr} is the reflected solar radiation,

Q_{lrbr} is the net longwave back radiation,

Q_{ehl} is the heat loss by evaporation ,

Q_{hcf} is the heat loss by conduction, biological processes etc.

Q_{sr} is given by $\beta S\cos(\sigma t)\cos(\lambda+\delta)$, $Q_{sr} > 0$ or otherwise zero (see Pugh and Rayner 1981, Sultan and Ahmad, 1993, Reeds ,1977, Reeds,1983, Gill, 1982) ,where β is the atmospheric extinction coefficient, which is approximately 0.7 for vertical transimission (Defant, 1961), S is the solar constant which is equal to $1390 Wm^{-2}$, σ is the solar angular speed, λ is the solar declinatin, δ is the station latitude. Since the creek is near the equator we set λ and δ equal to zero. Q_{rsr} is 10% of Qsr and may be negleted. $Q_{sr} = 180 Wm^{-2}$.

Using Brunts formula

$$Q_{lrbr} = 0.985\psi Tw^4(0.39-0.05e_a^{1/2})$$

where ψ is the Stefanal-Bolzman Constant. Tw is the water temperature, e_a is the vapour pressure of air in mb. Taking e_a, of 25 mb and Tw, of 25^0C, $Q_{lrbr} = 62 Wm^2$.

$Q_{ehl}=(11.2 +4.1W)(e_s-e_a)$ (see Pugh and Rayner ,1981),

where W is the wind speed in m s^{-1}, e_a is the air vapour pressure, and e_s is the saturated vapour air pressure at the sea temperature. Taking e_s at 33 mb (75% saturated at 25^oC and wind at zero, $Q_{ehl} = 90$ W m^{-2}.

$Q_{hcf} = 0.47(11.2 + 4.1W)(Ts-Ta)$ W m^{-2} ,

where Ts is the water temperature, and Ta is the air the air temperature.

Ts-Ta is 1.25 ^{o}C. $Q_{hcf} = 15$ W m^{-2}. The net heat balance becomes $Q_T = Q_{sr} - Q_{lrbr} - Q_{ehl} - Q_{hcf} = 180-62-90-15 = 13$W m^{-2}.

Q_T can be interpreted the heat flux (adv + diff) through the channel which thus can be calculated from the observations.

4.3.2 Advective and diffusive flux

The ebbing water must on average be warmer,by an amount δT, than the flood water. That is the net heat output by the water exchange equals the net heat gain from radiation. The net heat flux can be estimated from the sum of the advective and the diffusive flux ($Q_T = Q_{Tadv} + Q_{Tdif}$) as follows:

$Q_{Tadv} A_c = \rho c_p Q_e T_{o,}/A_c$ and

$A_C Q_{Tdif} = \rho c_p Q_{max} \delta T / A_C$

Q_{Tadv} is the advective heat flux, Q_{Tdif} is the diffusive heat flux, Q_{max} (aproximately Q_1 is the net volume flux, δT is the temperature difference from the creek and the ocean during North peak dry season. Q_e is the evaporative volume flux ,A_c is the surface area of the creek

heat of the sea water ,

$c_p = 4000$ J$(kg^oC)^{-1}$;$\rho = 1000$ kgm^{-3}, $Q_e = 1.6$ m^{3}s^{-1}, $T_o = 27.8^oC$, $A_c = 22 \times 10^6$ m^3.

$Q_{max} = 62 m^3 s^{-1}$, and $\delta T = 1.5^oC$

Therefore the value for advective heat flux $Q_{Tadv} = 6 Wm^{-2}$ (inwards) and diffusive heat flux $QT_{dif} = 17$ W m^{-2} (outwards) the net heat flux is 11W m^{-2}.

The results from the calculation of heat flux must be treated with great caution. It is based on measurements of temperature during day time,while during the night the difference in temperature is probably smaller (fig.10). The estimate of Q_{max} is also made on too few data and a not very precise estimate of Q_e . However, it indicates the correct order of magnitude of the heat flux or the budget equation qiven above.

Alternatively the heat flux can be calculated from the current meter data simply by using the formula :

$$Q_T = \int_\tau \rho c_p A_{xs} U(t) T(t) \tilde{c}$$

where U is velocity and T is temperature, and τ is the period of observation, which has to be of the order of the residence time.

4.4 The Bottom Layer at the Exchange Section

4.4.1 Estimations of friction velocity,drag coefficient and the depth of the boundary layer.

The pendelums measurements nearest to the bottom in the mid channel position (figs. 4.1.2a-b.) were placed 1, 2 , 3 and 4 (corresponding to pendelum # 20,19,18 and 17 in fig.2) meters from the channel-bed . These current measurements, made twice a month during three months at flood and ebb and at spring and neap periods, provide motivation for a simple study of the bottom friction layer. Fig.12. show some of the profiles of the measurments from the pendelums measurements From the profiles U(z) we try to determine the friction the bottom stress, the roughness depth and the quadratic drag coefficient and the depth of the logarithmic layer.

The expression for the friction layer is as follows:

$$U(z) = (U^*/k) \ln(z/z_0), \qquad 4.4.1a$$

where U(z) is the horizontal velocity profile in the boundary layer. U^* is the friction velocity and k is a universal constant known as von Karman's constant (0. 42). In our above interpretation

z is the vertical distance from the sea bed.

z_0 is the roughness length, which is a function the bottom stucture.

The friction velocity,U^* can be defined by the expression

$$U^* = \sqrt{\frac{\tau}{\rho}} \qquad 4.4.1b$$

from which

$$\tau = \rho U^{*2} \qquad 4.4.1c$$

where τ is the bottom shear stress and ρ is density of water.

The quadratic drag coefficient (C_d) is given by the expression,

$$\tau = \rho c_d U_o^2$$

where Uo is the velocity outside the boundary layer,

thus

$$c_d = \frac{\tau}{\rho U_o^2}$$

The above parameters were determined from a matlab program that estimates the friction velocity and roughness length by least square fit of the current data to the logarithmic profile (fig.12). This was done by rearranging equation 4. 4.1a as follows:

$$U(z) = \frac{U^*}{k} \ln z - \frac{U^*}{k} \ln z_o \quad ,$$

and performing linear regression to the straight line equation ;

$$y = mx + C \quad ,$$

where

$$\text{the slope} = \frac{U^*}{k},$$

$$\text{the intercept } C = -\frac{U^*}{k} \ln z_o,$$

and

$$z_o = e^{kc/U^*}.$$

U_o is the mean velocity in the layer above the friction layer and was estimated and used in the program for each set of measurments. Table 8 shows the values for the parameters.

4.4.5 The exponential depth scale of the bottom friction layer

Wang and Craig (1993), point out that the depth scale of the constant eddy viscosity layer (the bottom friction layer) can be calculated, if the frequency (ω) of the dominant tidal component and the eddy viscocity (μ) are known, from the expression

$$D = \sqrt{(\frac{2\mu}{\omega})}$$

where D is the exponential depth scale of the constant eddy viscousity layer, μ , the friction

coefficient . It should be noted that the eddy viscosity layer is above the constant shear stress layer (the logarithmic layer) of which length can be estimated as from 0-4m above the sea-bed.

Common representation of the interior eddy viscosity (Wang and Craig,1993) is $\mu=cU^*H$, where H is the depth of the water and U^* the friction velocity. c is a constant ranging from 0.01 to 0.1. From the logarithimic profiles (fig.12) , almost constant velocity occur in the range from near the surface to about 11m below the surface. The curves suggest that the depth of the constant eddy viscosity layer lies between 4m and 9m above the sea- bed. Thus conveniently chosing the value for c as 0.01 allows us to determine the value for D. When the values for U^* of 0.04m s^{-1} from previous calculation (assuming this is the value at the base of the eddy viscous layer) and H taken as 20 m coincinding with the general depth of the channel at the mooring site. The value for μ is found to be 0.0082 m^2s^{-1}. Wang and craig foud a value of 0.0028 $m^2s^{-1}$for similar system. When ω is taken as $2\pi/T$, where T is 12.42 hrs, the value for the depth of the eddy viscocity layer is 10.8 m, this is compares well with the values of 9m obtained by Wang and craig for similar system. This shows that the currents in the channel do reach constant values towards the surface. The observations also confirm that the position of RCMs 10 m was suitably selected and further that the three lowest pendelums were within the boundary layer.

It should also be noted that the depth of the constant eddy viscous layer can be taken as the height where the mean flow velocity in the upper layer drops to about 90% of it's value. In some cases the boundary layer never grows to its maximum steady state value because it's build up (growth) time is close to the tidal cycle i.e. the current switches direction before the boundary layer is fully developed.

The foregoing results apply for a single channel , it is therefore necessary to carry out a detailed study of bottom layer in various locations of the creek system in order to throw light into physical mechanism interlinking the diverse ecosystems.

5.0 CONCLUSIONS

This study focuses on Tudor creek and it's channel connection to the ocean ,an area located in Mid-Kenya coast in the Western Indian Ocean. It emphasises the hydrology and hydrodynamics of the system. Observations and results lead to the following conclusions:

1. Tides are semidiurnal of form number 0.18, including a minor phase difference between the creek area and the ocean.
2. The mean spring tidal range 3.1m at the entrance.
3. Typical flood tide lasts 6.5h while ebb tide extend for 6.3h. Mean flood and ebb currents are 0.36 ms^{-1} and 0.40 ms^{-1}.
4. The mean flux of the water during ebb and flood was determined from current meter measurements to 2500 and 2700 m^3s^{-1}respectively.Tide gauge observations indicate a mean flow of 2600m^3s^{-1}.
5. The advective heat flux through the Tudor channel is 11 W/m^2 outward during PDS (advective heat flux into Tudor creek is 6 W/m^2 and the outward diffusive heat flux is 17 W/m^2.
6.The longitudinal salinity gradient from the creek to the entrance show mean salinity and temperature ranges from 35.49 PSU,27.90^oC to 35.19 PSU ,27.24^oC and 35.60 PSU,29.36^oC to 34.68 PSU, 27.80^oC for South east and North east peak dry periods.

7. The residence time is of the order of two weeks.

8. The friction velocity was found to be 0.04 ms^{-1} leading to a drag coefficient value of 0.008 x 10^{-3}.The roughness length was 0.34m and the depth of constant eddy viscosity layer was estimated to 10.8m.

9. There seems to be very little asymmetry in the tide of the creeks but the velocity measurments indicate an interesting asymmetry in the channel.

There is still much room for further studies of the hydrodynamics of the system combined with modelling. It is necessary to study the water exchange (flushing) in detail as the present results are not conclusive. Other objectives may include a more detailed study of the bottom boundary layer and the link between the system and the adjacent lagoons or reef waters as this may be important for the chemical and biological processes.

ACKNOWLEDGEMENTS

I am very grateful to Drs. Lars Rydberg and Ulf Cederlöf for valuable lecturing , assistance in field work and supervision in writing this manuscript. I also thank the staff members of the Department of Oceanography, Göteborg University and lab attendants of Kenya Marine and Fisheries Research Institute (K.M.F.R.I.) for helping me in one way or the other.

In particular, special thanks go to the Director of K.M.F.R.I. Dr. E. Okemwa and Dr. O. Linden, the coordinator within the Swedish Agency for Research Cooperation with Developing Countries (SAREC) for their effort in initiating a research programme in the East African region, without which this work would not have been possible.

This work was supported by by the Swedish Agency for Research Cooparation with Developing Countries (SAREC).

REFERENCES

Defant A. (1961) Physical Oceanography. Vol.2. Pergamon Press, New York. 590pp.

Griffiths J.F. (1972) Climate. In: East Africa: its People and Resources. W.T.W. Morgan,editor. Oxford University Press. pp.106-117.

Gill, A.E., (1982) Atmosphere - ocean Dynamics, Academic press, San Diego, calif. 662pp.

Haamer, J. (1974) Current measurements using gelatin pendulums. Vatten 1.79 (in Swedish).

Norconsult M.S. (1975) Water Pollution Study in Mombasa. Sewage Dissposal Project. Vol.5 .

Odido, M. O.,(1994) Tidal Dynamics of Tudor creek,Mombasa ,Kenya. Msc. Thesis, Gothenberg, 1994.

Schauer U. (1987) Determination of bottom boundary layer parameters at two shaloow sea sites using the profile method. Continental Shelf Research . 7(10),1121-1230.

Reeds,R.K., (1977) On estimating insolation over the ocean. Journal of Physical Oceanography 7, 482-485.

Reeds,R.K,(1983) Heat fluxes over the eastern Pacific and aspects of the 1972 El Nino. Journal of geophysical research 88,9627-9638

Sultan S.A.R. and Ahmad (1993) Surface and oceanic heat fluxes in the Gulf of Oman. Continental Shelf Research. 13(10),1103-1110.

Pugh, D.T. and Rayner , R.F.,(1981) The tidal regimes of three indian ocean atolls and some ecological implications.Estuarine coastal and Shelf science 13,389-407.

Ulf Cederlof, (1993) Post graduate lecture notes in Advanced Fluid Mechanics (with some application of matlab techniques for time series analysis) , Department of Oceanography, Goteborg University.

Wang X.H. and P.D.Craig (1993) An analytical model of tidal circulation in a narrow estuary. Journal of Marine Research. 51,447-465.

Wolanski E. (1985) An evaporation-driven salinity maximum Zone in Austalia Tropical Estuaries. Estuarine and Coastal Shelf Science

Wolanski, E. (1989) Measurments and modelling of Water circulation in mangrove swamps. UNESCO-COMARAF serie Documentaire No.3 43pp.

Wolanski,E., M.Jones and J.S.Bunt, (1980) Hydrodynamics of a tidal creek swamp system. Austalian Journal of Freshwater Research 31,431-450.

Wolanski,E.,Y. Mazda, B. King and S.Gay, (1990) Dynamics, Flushing and trapping in Hichnbrook Channel, Coast. shelf science 31,55-580.

TABLES

Table 1. List of some tidal constituents

Names of partial tide	Symbol	period(hours)
Semi-diurnal Components		
(1) Principal Lunar	M2	12.42
(2) Principal Solar	S2	12.00
(3) Luni-Solar Semi-diurnal	K2	11.97
(4) Luni elliptic		12.19
Diunal Components		
(5) Luni -Solar Diurnal	K1	23.93
(6) Principal Lunar Diurnal	O1	25.82
(7) Principal Solar Diurnal	P1	24.07
Shallow Water Tides		
	$2SM_2$	11.61
	M_4	6.21
	MS_4	6.10
	S_4	6.00
	M_6	4.14
	$2MS_6$	4.09

Table 2. Classification of Tides according to F-ratio

Species	Value of F
Semi-diurnal	$0 < F < 0.25$
Mixed, Mainly Semi-diurnal	$0.25 < F < 1.5$
Mixed, Mainly diurnal	$1.5 < F < 3.0$
Diurnal	$F > 3.0$

Table 3. Harmonic analyses of Tudor creek (KMC) and oceanic (Mackenzie point) .

	Tudor creek			Oceanic (Mackenzie Point)		Kilindini Creek (Pugh, 1979)	
κ	T	ς	Φ	ς	Φ	ς	Φ
M2	12.42	1.0648	112.4450	0.9666	109.0059	1.055	0
S2	12.00	0.5412	-26.9679	0.5053	-28.2234	0.521	-7.7
N2	12.66	0.1949	139.7338	0.1800	141.0911	0.201	10.22
K2	11.97	0.1389	-77.1642	0.1374	-96.9357	0.139	-7.72
K1	23.93	0.2241	-03.8855	0.1843	-20.3187	0.191	20.02
O1	25.84	0.0886	-13.6574	0.0757	-12.4259	0.113	21.02
P1	24.07	0.1500	111.2500	0.1621	90.8322	0.055	20.28

κ=Constituent , T=Period , ς=Amplitude(meters), Φ= Phase(in degrees)

Table 4. Harmonic analyses of Tudor creek (KMC) and oceanic (Mackenzie point) .

	Tudor creek			Oceanic (Mackenzie Point)		Kilindini Creek (Pugh, 1979)	
κ	T	ς	Φ	ς	Φ	ς	Φ
M2	12.42	1.0648	112.4450	0.9666	109.0059	1.055	0
S2	12.00	0.5412	-26.9679	0.5053	-28.2234	0.521	-7.7
N2	12.66	0.1949	139.7338	0.1800	141.0911	0.201	10.22
K2	11.97	0.1389	-77.1642	0.1374	-96.9357	0.139	-7.72
K1	23.93	0.2241	-03.8855	0.1843	-20.3187	0.191	20.02
O1	25.84	0.0886	-13.6574	0.0757	-12.4259	0.113	21.02
P1	24.07	0.1500	111.2500	0.1621	90.8322	0.055	20.28

κ=Constituent , T=Period , ς=Amplitude(meters), Φ= Phase(in degrees)

Table 5. Harmonic analyses for RCM93 at mid-channel depth 10 meters.

	U-component			V-component	
κ	T	ς	Φ	ς	Φ
M2	12.42	27.76	0	16.22	0
S2	12.00	14.56	9.99	9.45	9.96
N2	12.66	5.70	12.47	3.37	12.51
K2	11.97	2.83	1.2	2.10	2.31
K1	23.93	1.29	19.7	1.24	22.25
O1	25.84	2.00	12.46	1.10	15.25
P1	24.07	3.52	1.00	1.72	2.62

κ=Constituent , T=Period , ς=Amplitude(meters), Φ= Phase(in degrees)

Table 6. Mean salinities and mean temperatures in SEM PDS 1992 and NEM PDS 1993.

Period	Sept-Nov	Feb-Apr	May	Nov-Dec
	SEM PDS	NEM PDS	PLRS	PSRS
	1992	1993	1993	1992
Kombeni	34.41	35.61	33.28	34.81
River stn #1	(35.07-34.07)	(35.21-35.15)		
	27.61 C	30.2 C		
Creek stn 2,3,4&5	35.49	35.60	34.42	35.33
	(35.35-35.63)	(35.81-35.38)		
	27.90	29.36		
Entrance st #6,7	35.19	34.68	34.85	35.36
	(35.14-35.23)		(34.63-34.73)	
	27.24		27.80	

Acronyms used in the table: SEM PDS , south east monsoon peak dry season
: NEM PDS,north east monsoon peak dry season
: PLRS,peak long rain sesson
: PSRS, peak short rain season

Table7. Hydaulic characteristics of Tudor creek.

Period	Stations	
	Inside creek (KMC)	**Entrance Mckenzie pt.**
	(Tidal Range in Meters)	(Tidal Range in Meters)
Spring	3.12	2.76
Neap	0.91	0.86
Mean	2.21	1.98
Mean flood range	--------	2.00
Mean ebb range	--------	1.98
Mean flood period	6h 28min	6h 20min
Mean ebb period	5h 56min	6h 5min
	Time of High Water (HW)	12.40h
12.39h		
Time of Low Water (LW)	12.38h	12.39h

Table 8. Friction layer parameters for Tudor channel

Date	Uo m s^{-1}	U* m s^{-1}	z_o m	c_d
27/10/92	0.45	0.044	0.480	0.0096
	0. 48	0.055	0.370	0.0150
14/10/92	0.37	0.032	0.159	0.0076
	0.43	0.044	0.339	0.0106
11/11/92	0.43	0.038	0.361	0.0077
26/11/92	0.44	0.039	0.374	0.0080
	0.46	0.041	0.305	0.0079
	0.45	0.041	0.338	0.0082
11/1/93	0.45	0.039	0.316	0.0075
	0.50	0.040	0.275	0.0067
Mean values	0.44	0.041	0.335	0.0088

FIGURE CAPTIONS

Figure 1. The study area - Tudor creek system showig the location of stations numbered 1 to 7 the tide gauges and the current meters and the hydrographic sections.

Figure 2. Mooring arrangements for the pendulum current meters and the recording current meter(s) RCM(s).

Figure 3. Uncorrected time series plots from tide gauge (a) at the entrance near the ocean (b) in the Tudor creek , corrected (spline-fitted) time series plots from tide gauge (c) at the entrance and (d) in the creek.

Figure 4. Stick diagrams for (a) recording current meter (RCM93) and (b) recording currennt meter (RCM94) (c) histograms showing the direction of the recording current meters

Figure 5. Energy spectra plots for (c) RCM93 and (d)RCM94.

Figure 6. Residual tidal currents in (a) the creek and (b) at the oceanic side; time series plots for the along channel component of (v) and the (u) current components for recording current meters(RCMs) (a) RCM93 (b) RCM94

Figure 7. A few extracted current record data (a) RCM94 and (b) tide gauge inside the creek (c) fig. from Wolanski Model on current and tide gauge data.

Figure 8. Hypsographic curve for the tide gauge station (a) inside the creek and showing the amount of water contained within the tidal area as a function of water level (b) time plot of volume flux obtained using the cross-section

Figure 9. Seasonal variation of temperature and salinity in Tudor creek.

Figure 10. Time series plot of temperature from tide gauge (a) in the creek ,(b) at the entrance and from (c) RCM93 and (d) RCM94.

Figure 11. Schematic diagram for (a) classical estuarine circulation (b) inverse estuarine circulation.

Figure 12. Part of the logarithmic profiles for (a) the pendulum current meters from near the surface to near the sea-bed (b) the lowest four pendulum meters.

Figure 1.

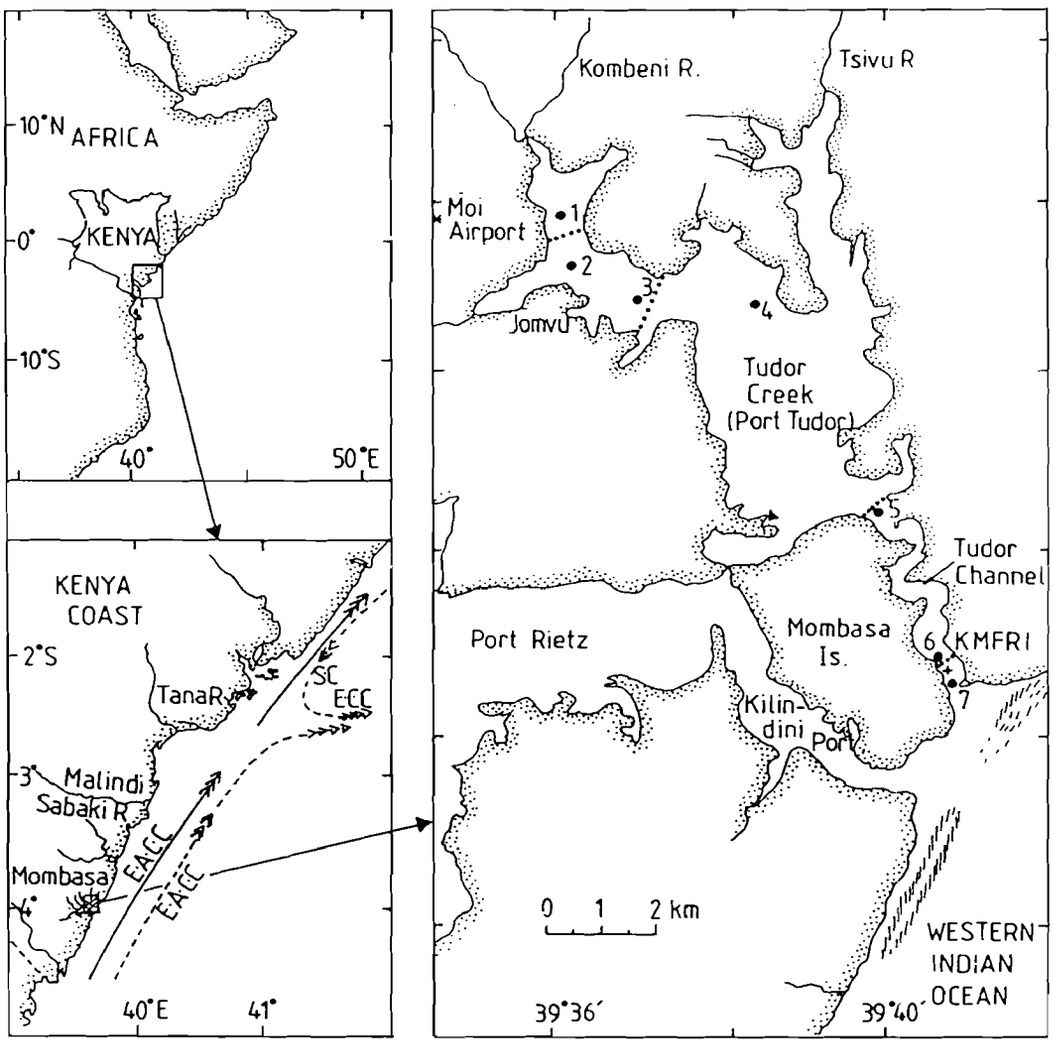

Fig. 1 MAP OF THE STUDY AREA
(TUDOR CREEK SYSTEM)

→→→ SE monsoon surface currents
---→→→ NE monsoon surface currents
E·A·C·C East African Coastal Current
E·C·C Equatorial Counter Current
S·C Somali Current
KMFRI Kenya Marine and Fisheries Research Institute

Key: ▵ Pressure gauge
• Oceanographic stations
* Meteorological stations
···· Oceanographic sections
//// Coral reefs
+ Recording current meter(s) station and pendelums

Figure 2.

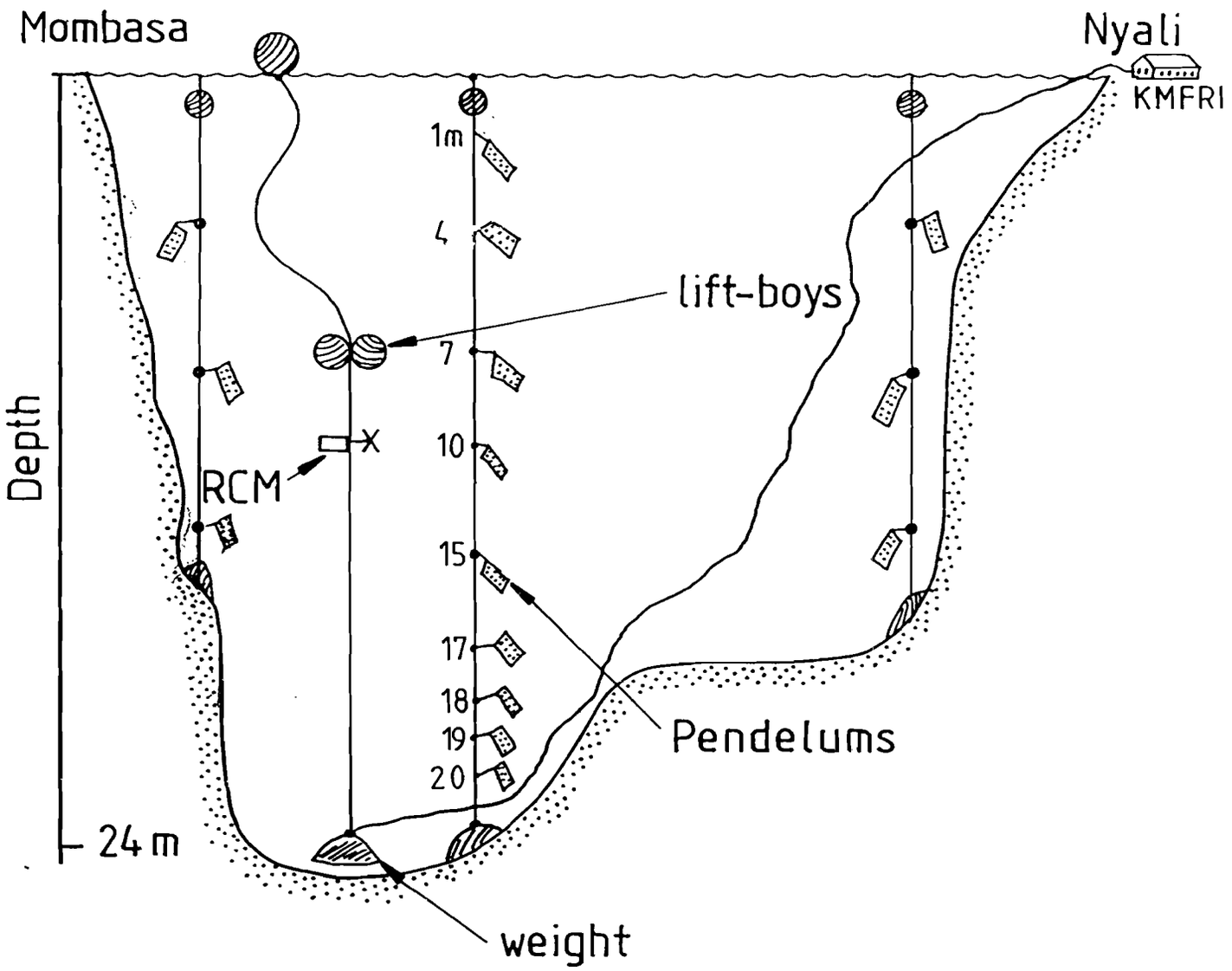
Mombasa
Nyali
KMFRI
1m
4
lift-boys
7
10
RCM
15
17
18
19
20
Pendelums
Depth
24 m
weight

Figure 3.

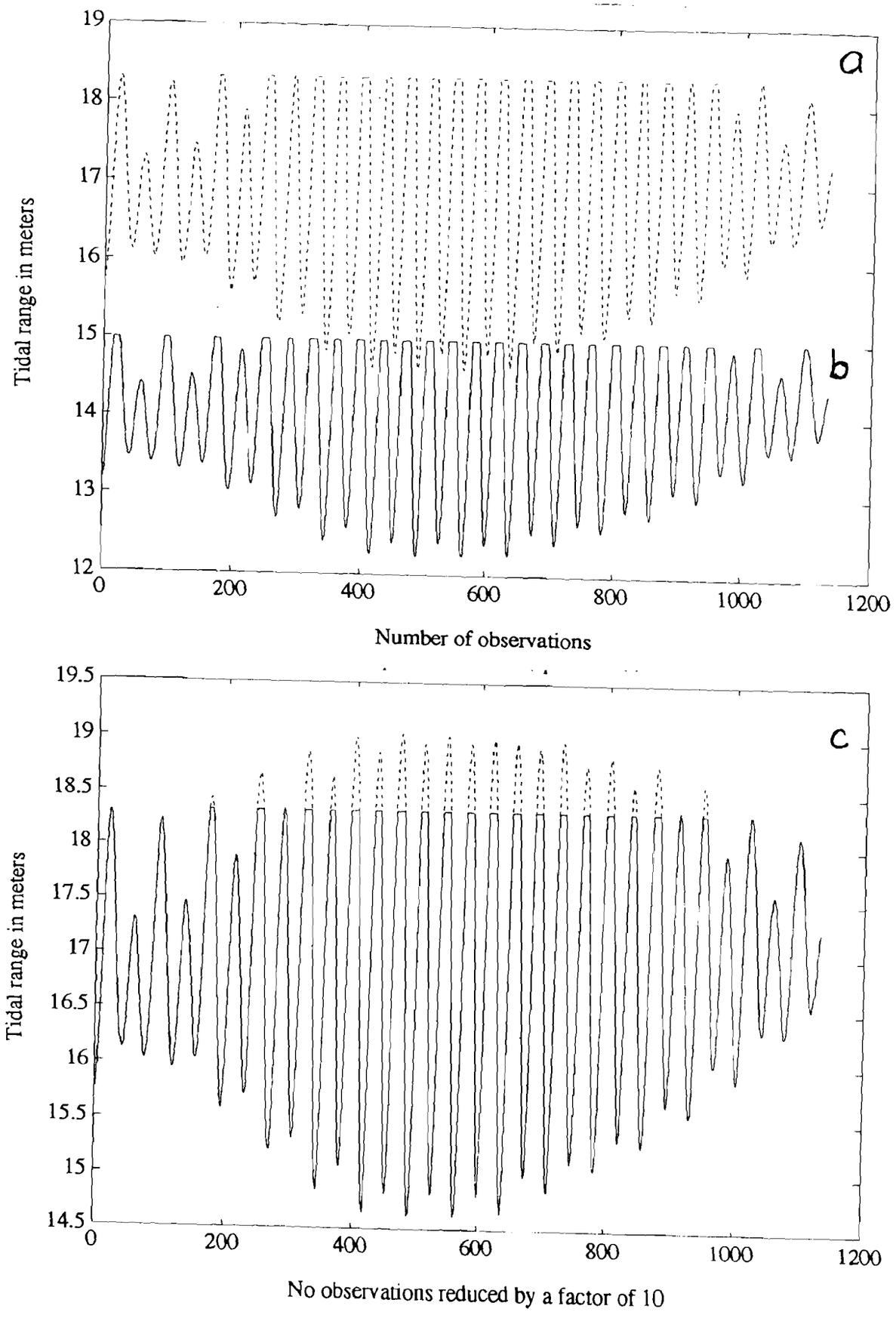
a
b
c
Tidal range in meters
Number of observations
No observations reduced by a factor of 10
19
18
17
16
15
14
13
12
19.5
18.5
17.5
16.5
0
200
400
600
800
1000
1200

Figure 3.

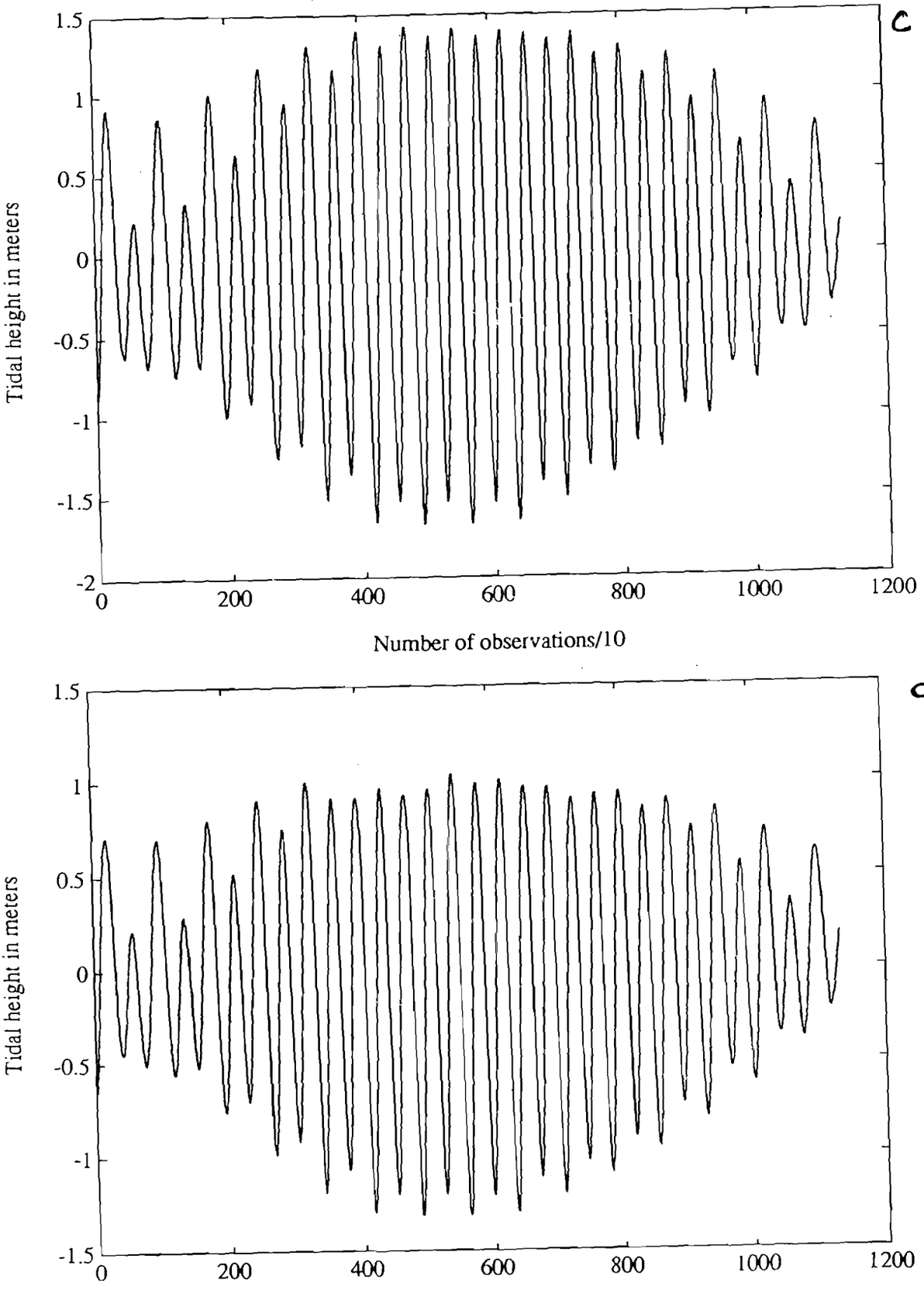
c
d
Tidal height in meters
Number of observations/10
1.5
1
0.5
0
-0.5
-1
-1.5
-2
0
200
400
600
800
1000
1200

Figure 4. a

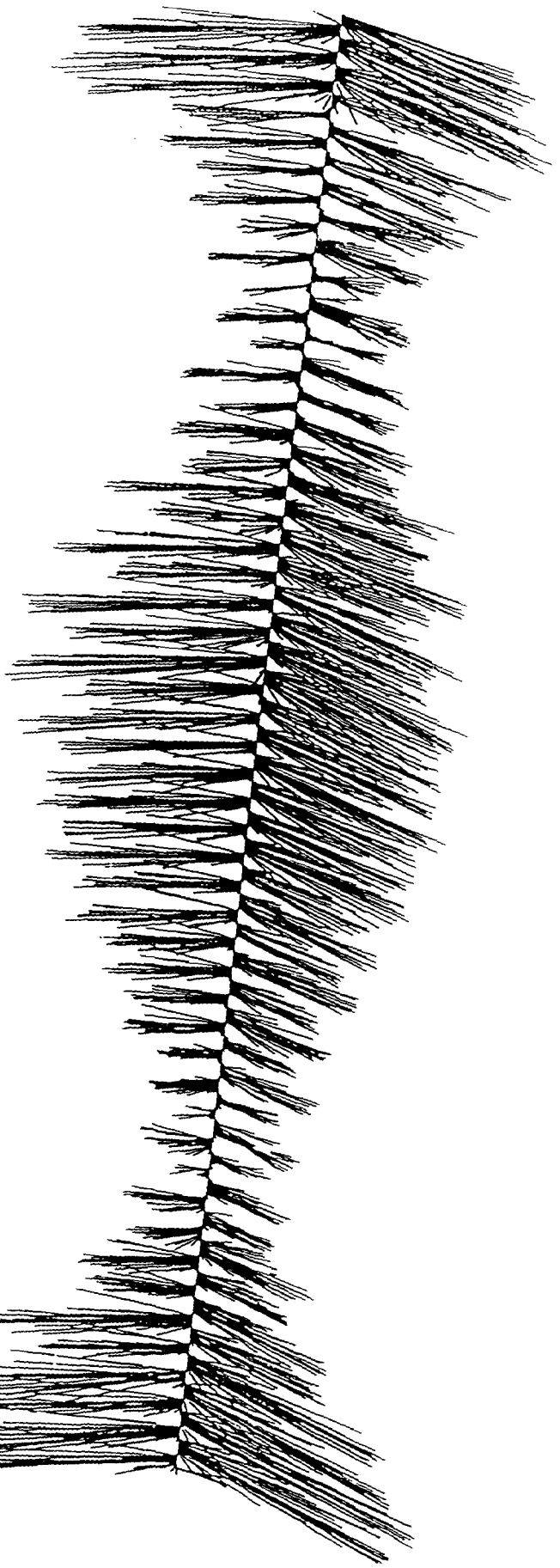

RCM-93

Figure 4. b

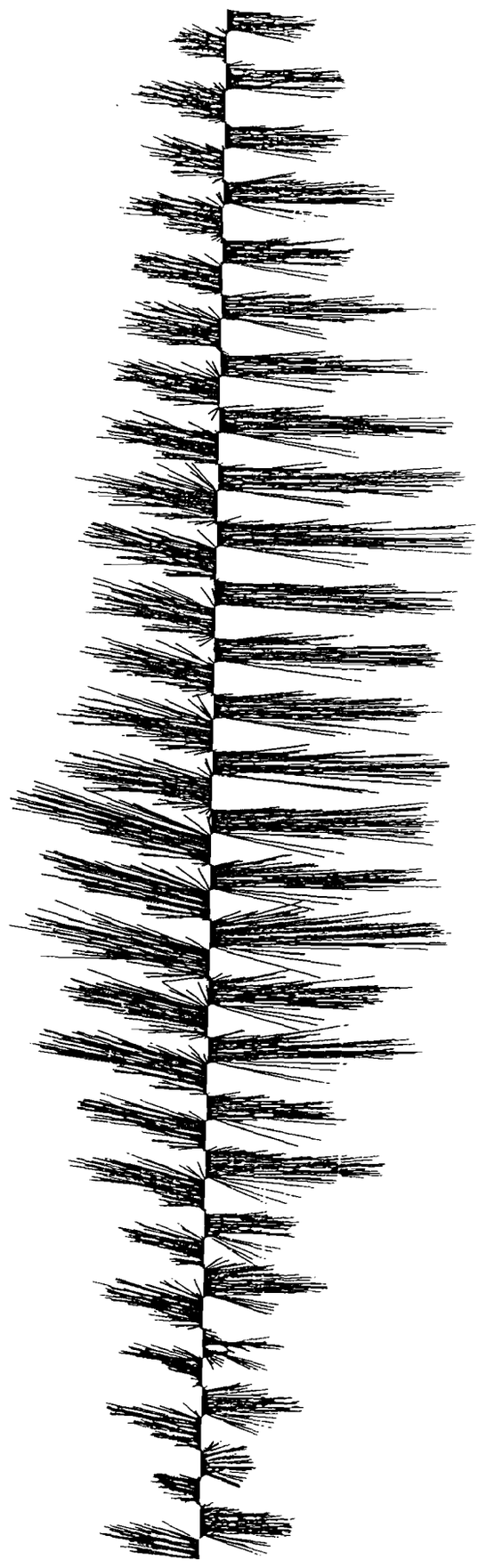

RCM-94.

20 cm/s

Figure 4.

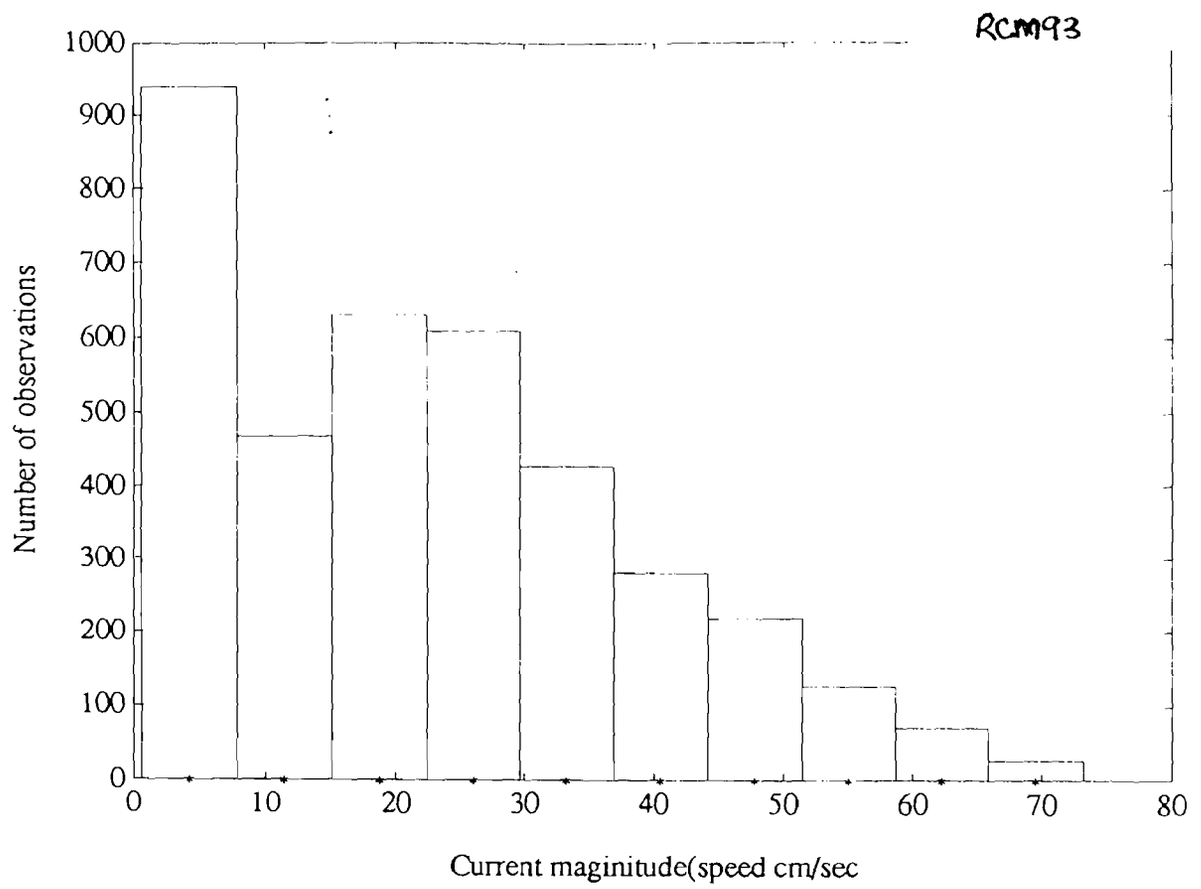
RCM93
C
Number of observations
Current maginitude(speed cm/sec
0
100
200
300
400
500
600
700
800
900
1000
0
10
20
30
40
50
60
70
80

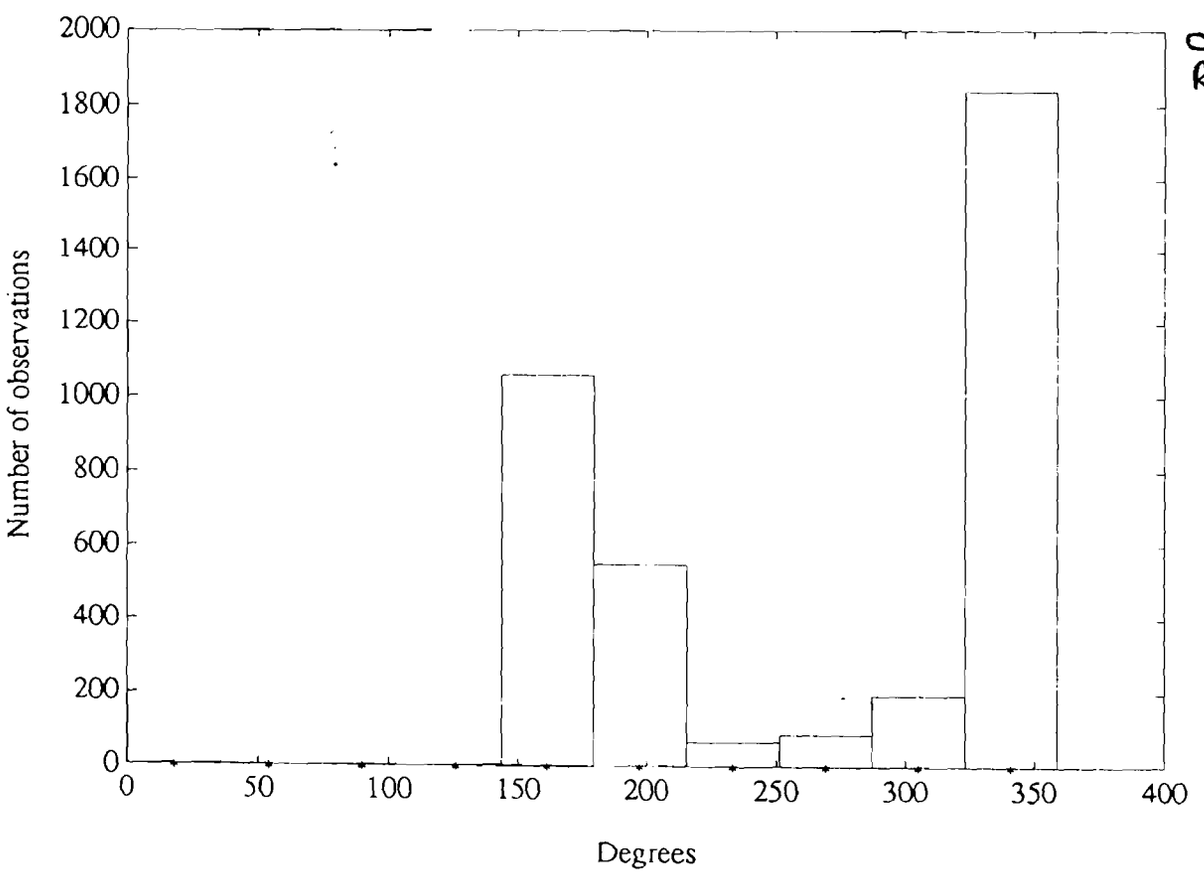
d
RCM 94
Number of observations
Degrees
0
200
400
600
800
1000
1200
1400
1600
1800
2000
0
50
100
150
200
250
300
350
400

Figure 5.

a

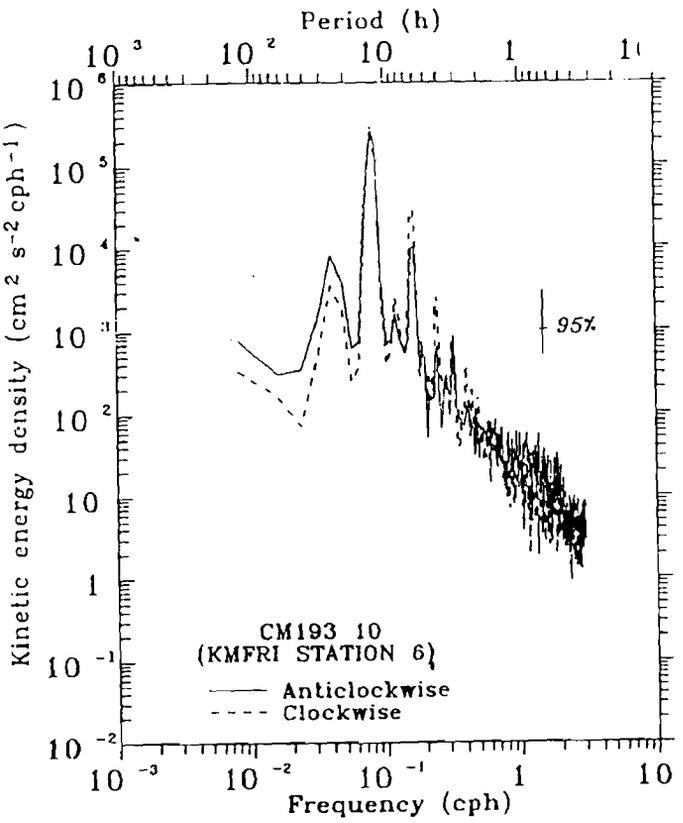
Period (h)
Kinetic energy density (cm² s⁻² cph⁻¹)
95%
CM193 10
(KMFRI STATION 6)
Anticlockwise
Clockwise
Frequency (cph)

b

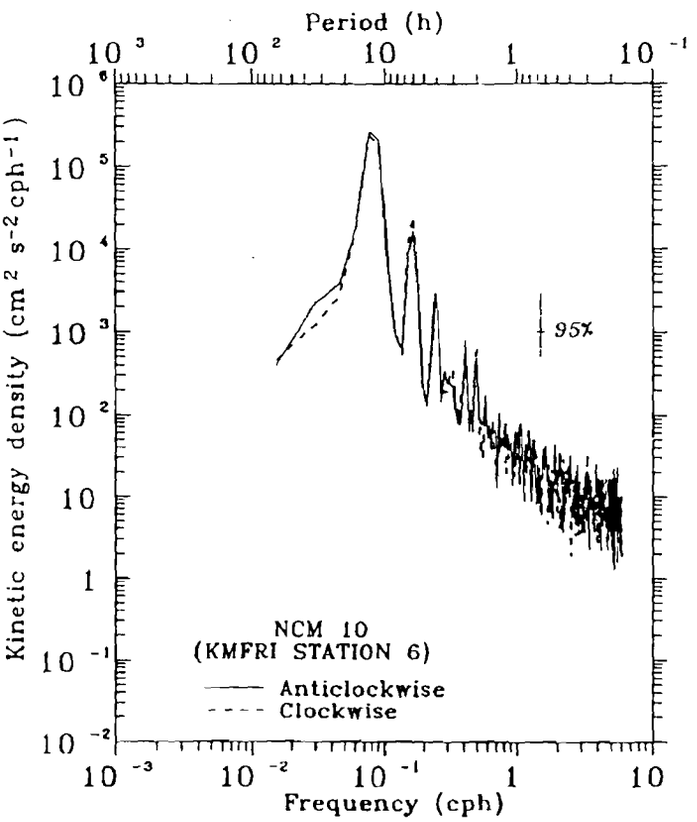
Period (h)
Kinetic energy density (cm² s⁻² cph⁻¹)
95%
NCM 10
(KMFRI STATION 6)
Anticlockwise
Clockwise
Frequency (cph)

Figure 6.

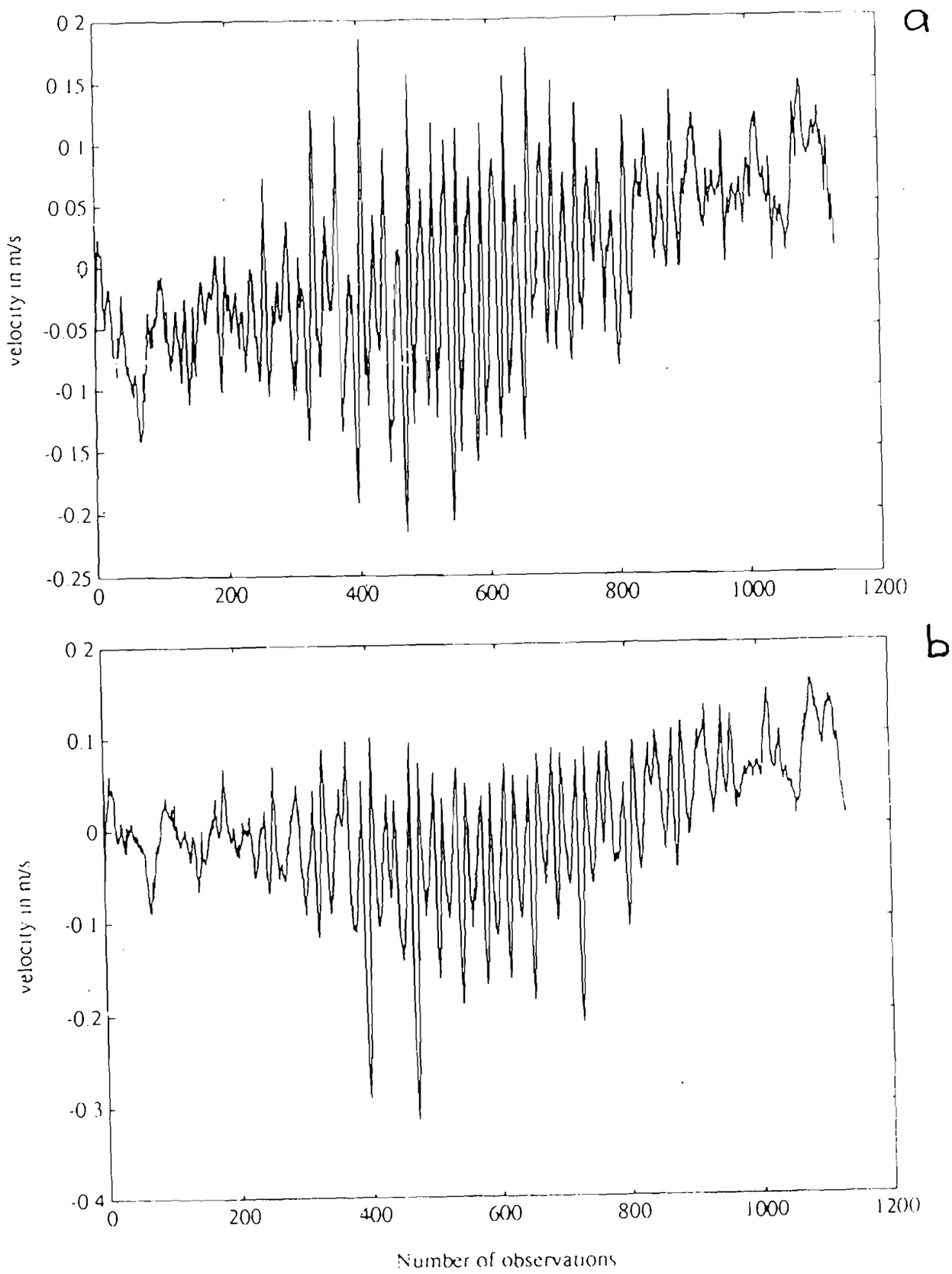
a
b
velocity in m/s
velocity in m/s
0.2
0.15
0.1
0.05
0
-0.05
-0.1
-0.15
-0.2
-0.25
0.2
0.1
0
-0.1
-0.2
-0.3
-0.4
0
200
400
600
800
1000
1200
Number of observations

Figure 6.

C

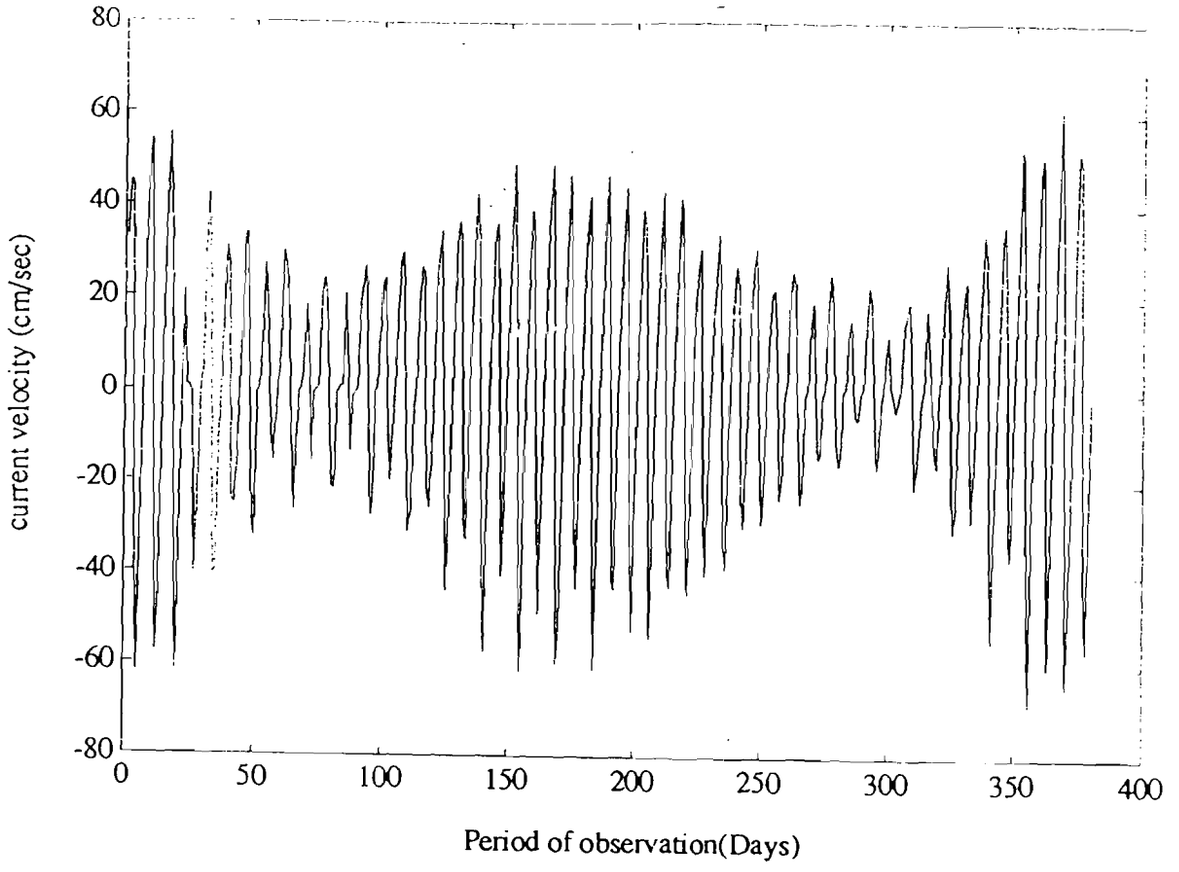
80
60
40
20
0
-20
-40
-60
-80
current velocity (cm/sec)
0
50
100
150
200
250
300
350
400
Period of observation(Days)

Figure 7.

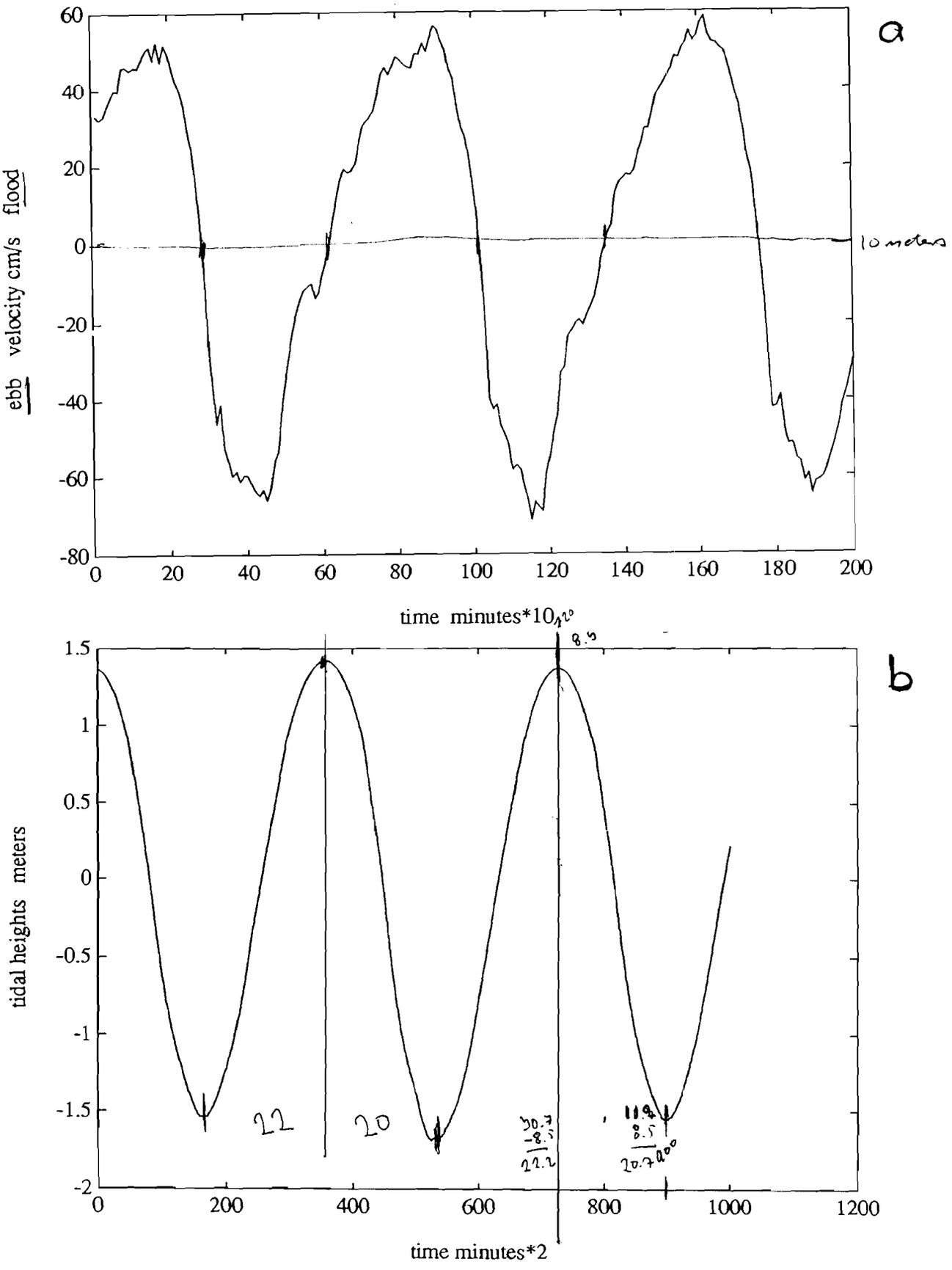
a
ebb velocity cm/s flood
10 meters
time minutes*10
b
tidal heights meters
time minutes*2

Figure 7.

C.

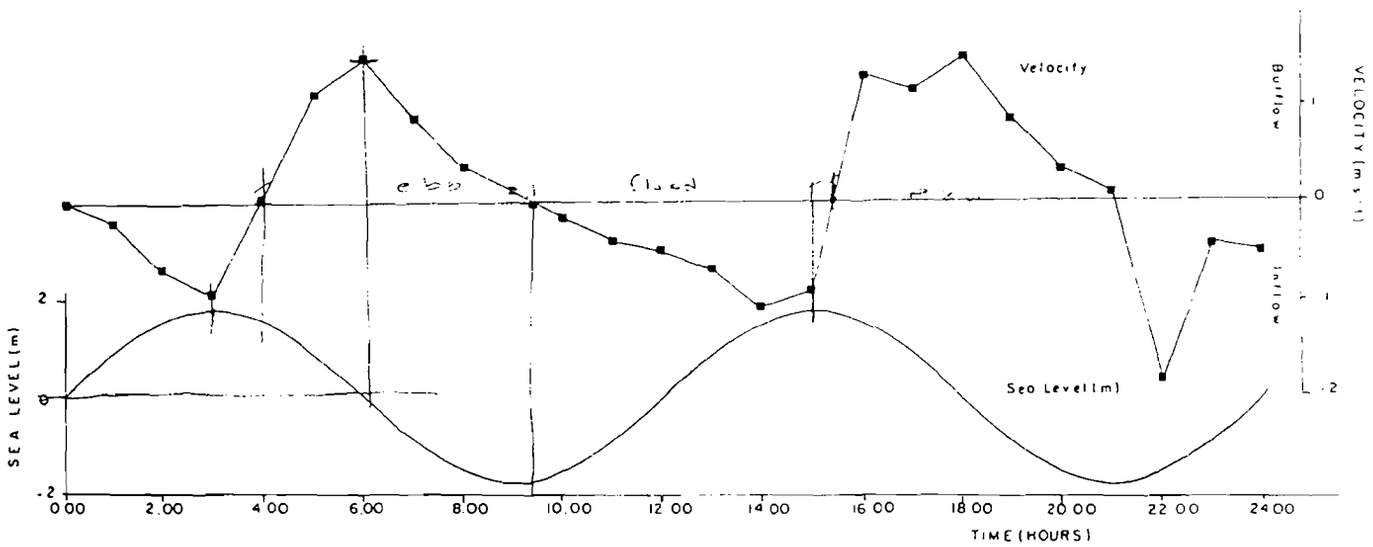
Velocity
Sea Level (m)
SEA LEVEL (m)
VELOCITY (m s⁻¹)
Inflow
Outflow
2
0
-2
1
0
1
2
0.00
2.00
4.00
6.00
8.00
10.00
12.00
14.00
16.00
18.00
20.00
22.00
24.00
TIME (HOURS)

Figure 8.

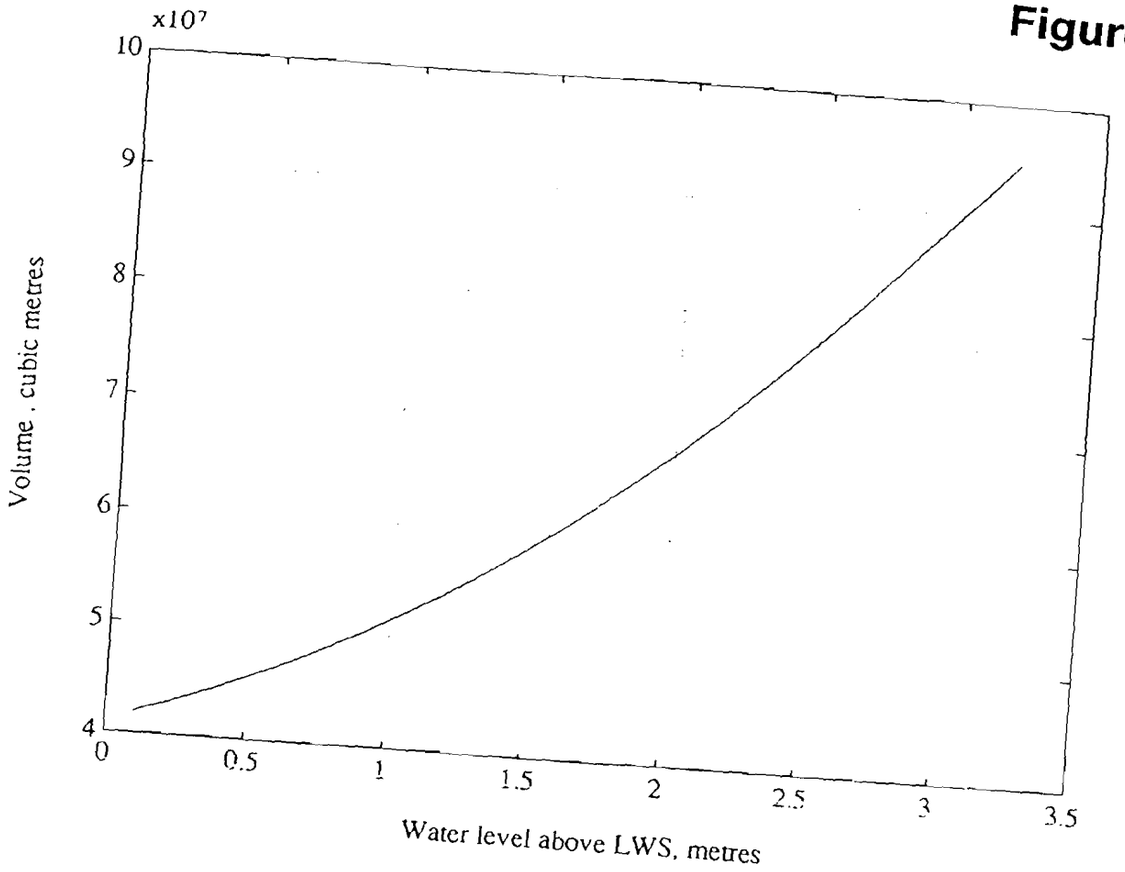
x10⁷
10
9
8
7
6
5
4
0
0.5
1
1.5
2
2.5
3
3.5
Volume , cubic metres
Water level above LWS, metres

a

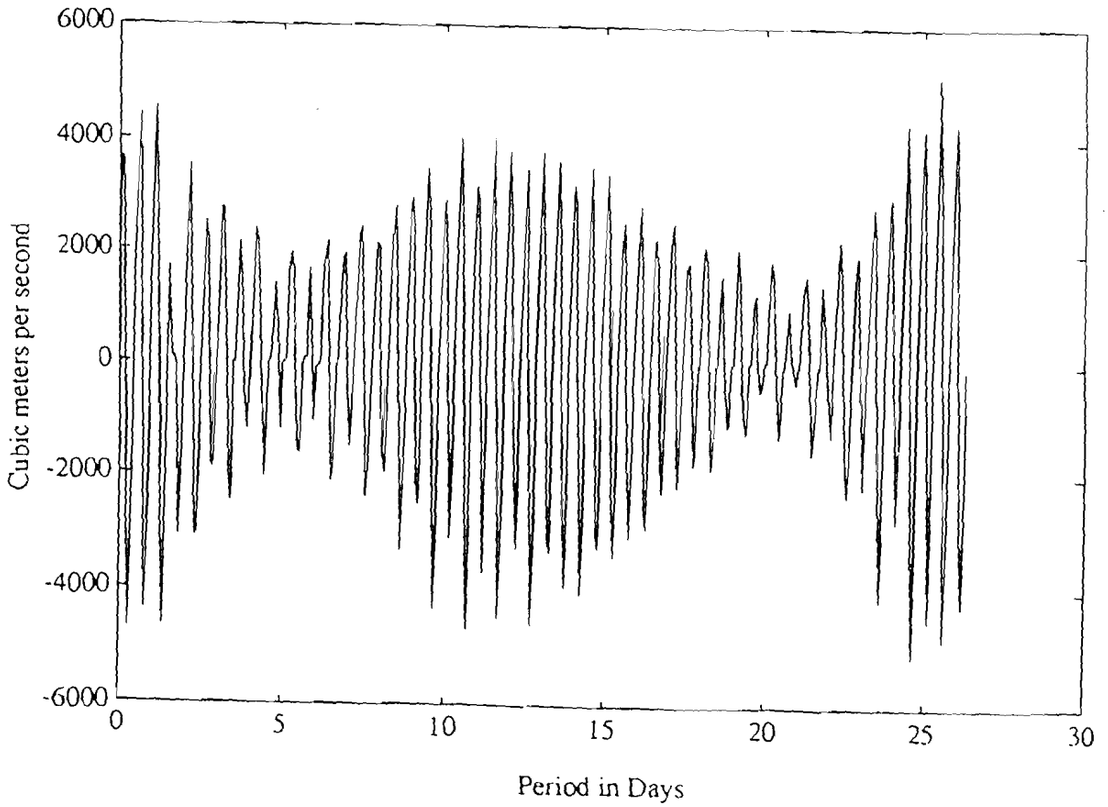
6000
4000
2000
0
-2000
-4000
-6000
0
5
10
15
20
25
30
Cubic meters per second
Period in Days

b

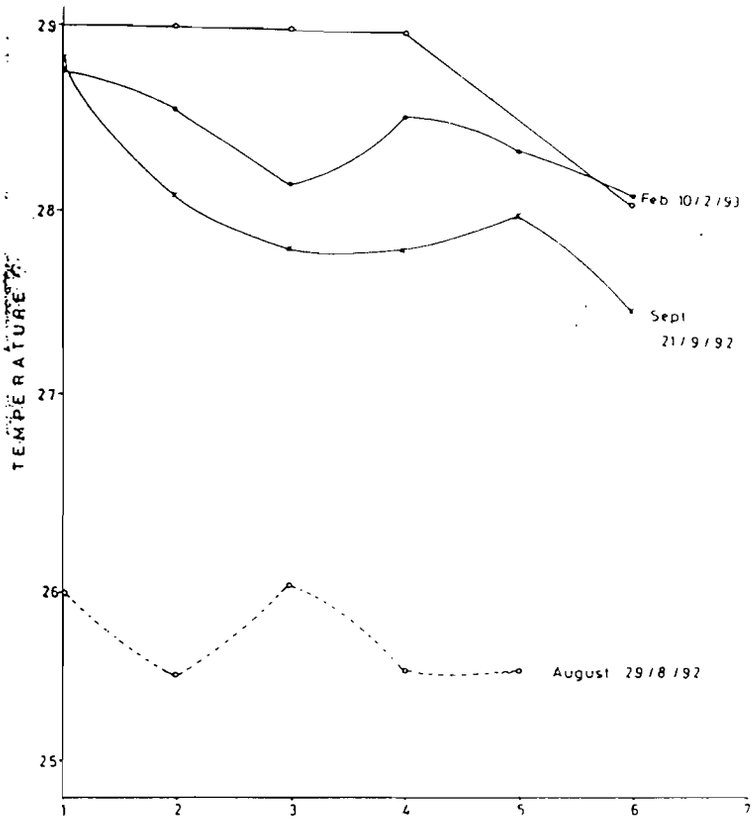
TEMPERATURE °C
29
28
27
26
25
1
2
3
4
5
6
7
Feb 10/2/93
Sept
21/9/92
August 29/8/92

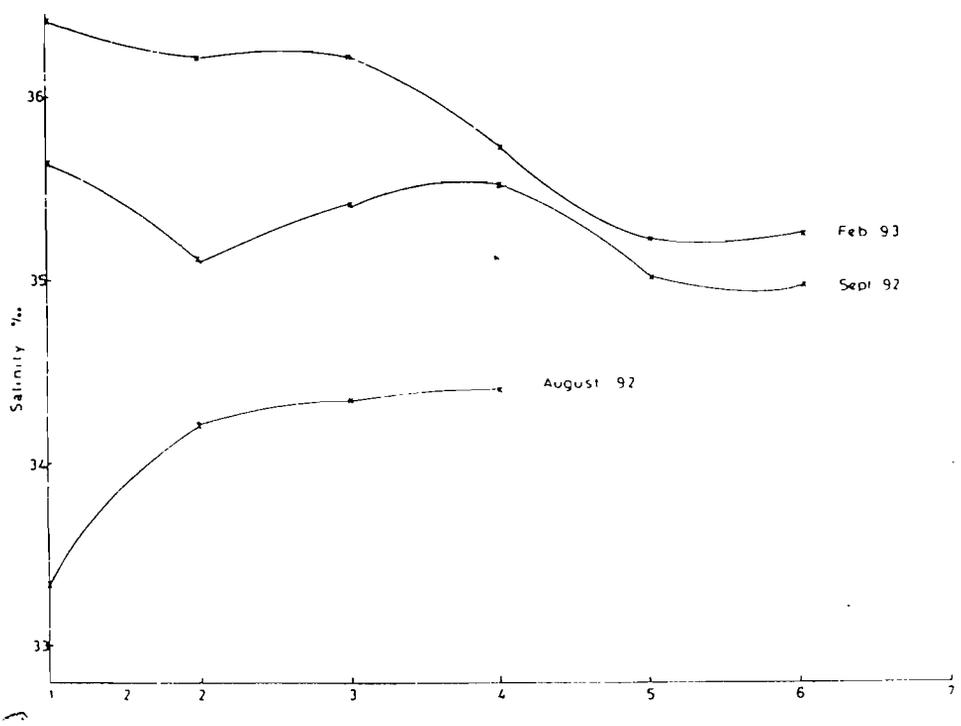
Salinity ‰
36
35
34
33
1
2
2
3
4
5
6
7
Feb 93
Sept 92
August 92

Figure 9.

Figure 10.

a

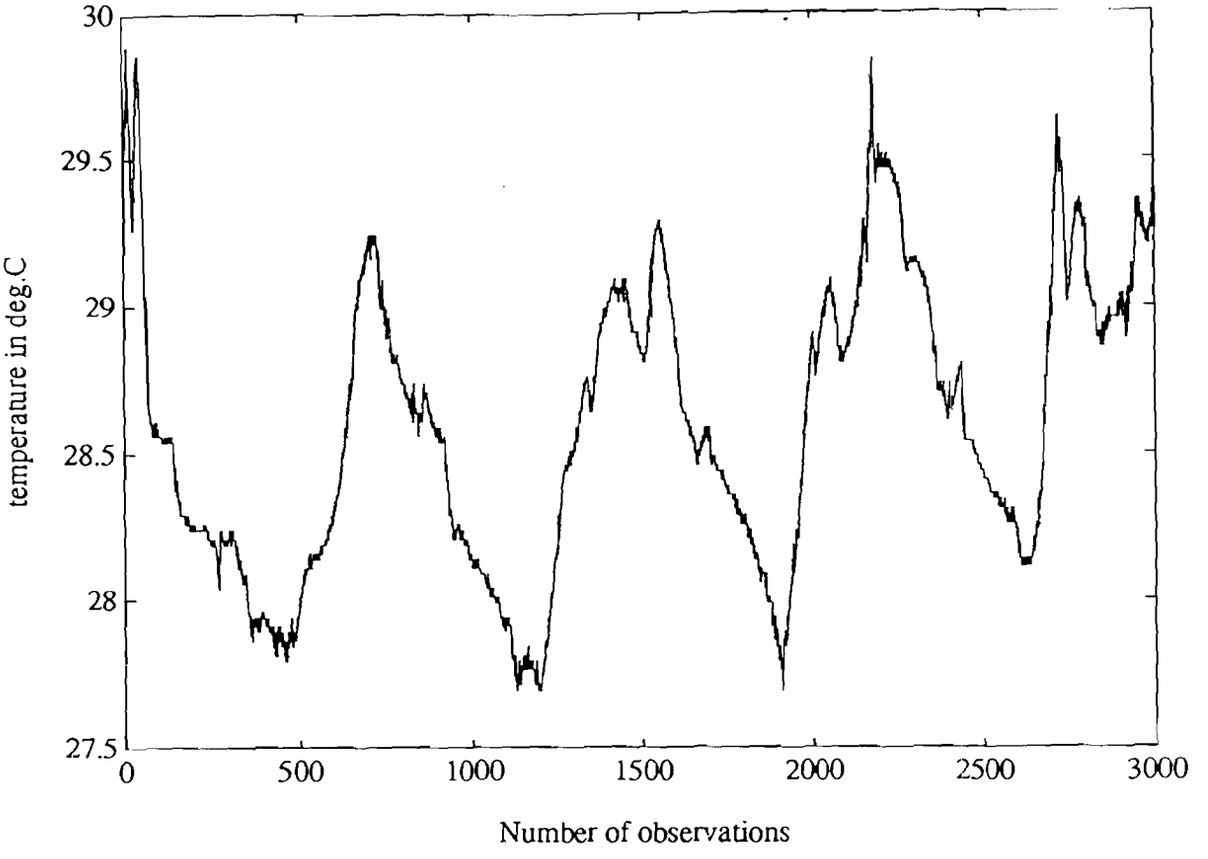
30
29.5
29
28.5
28
27.5
temperature in deg.C
0
500
1000
1500
2000
2500
3000
Number of observations

b

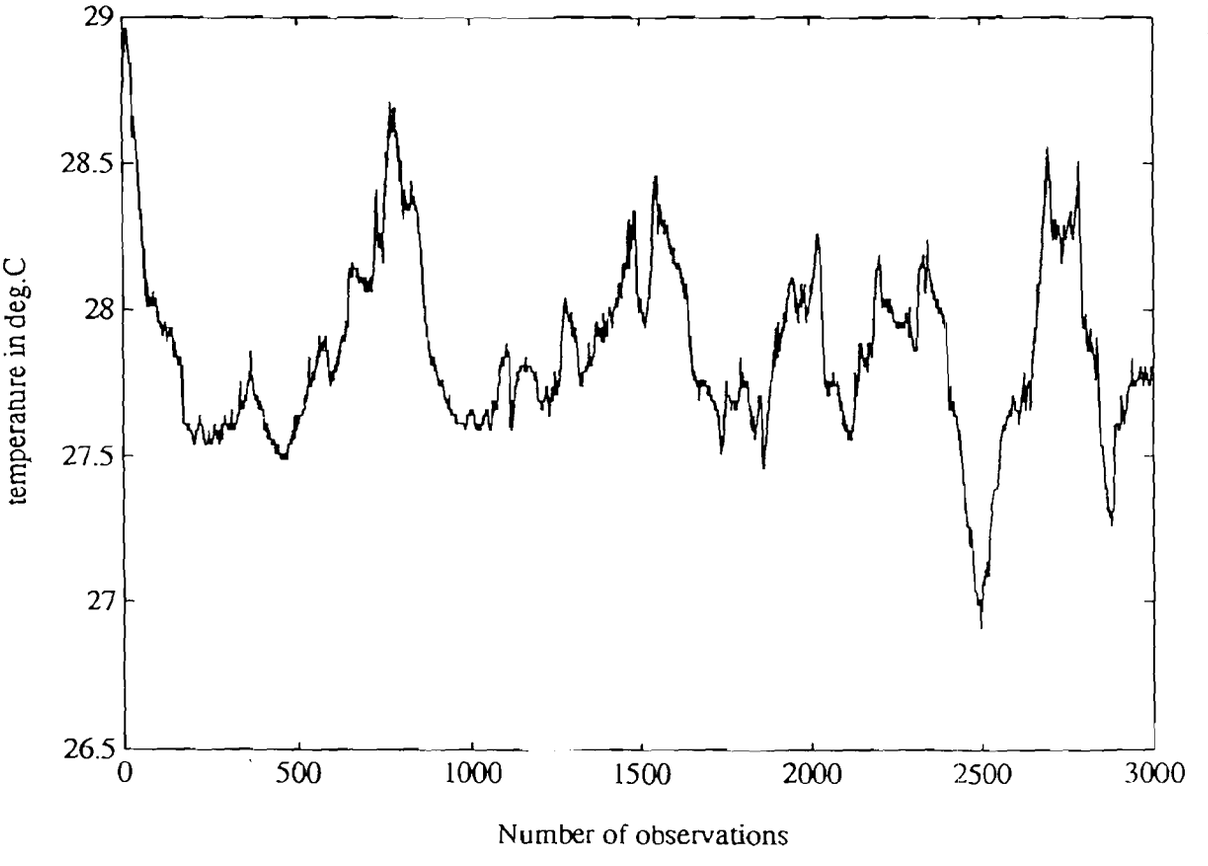
29
28.5
28
27.5
27
26.5
temperature in deg.C
0
500
1000
1500
2000
2500
3000
Number of observations

Figure 11.

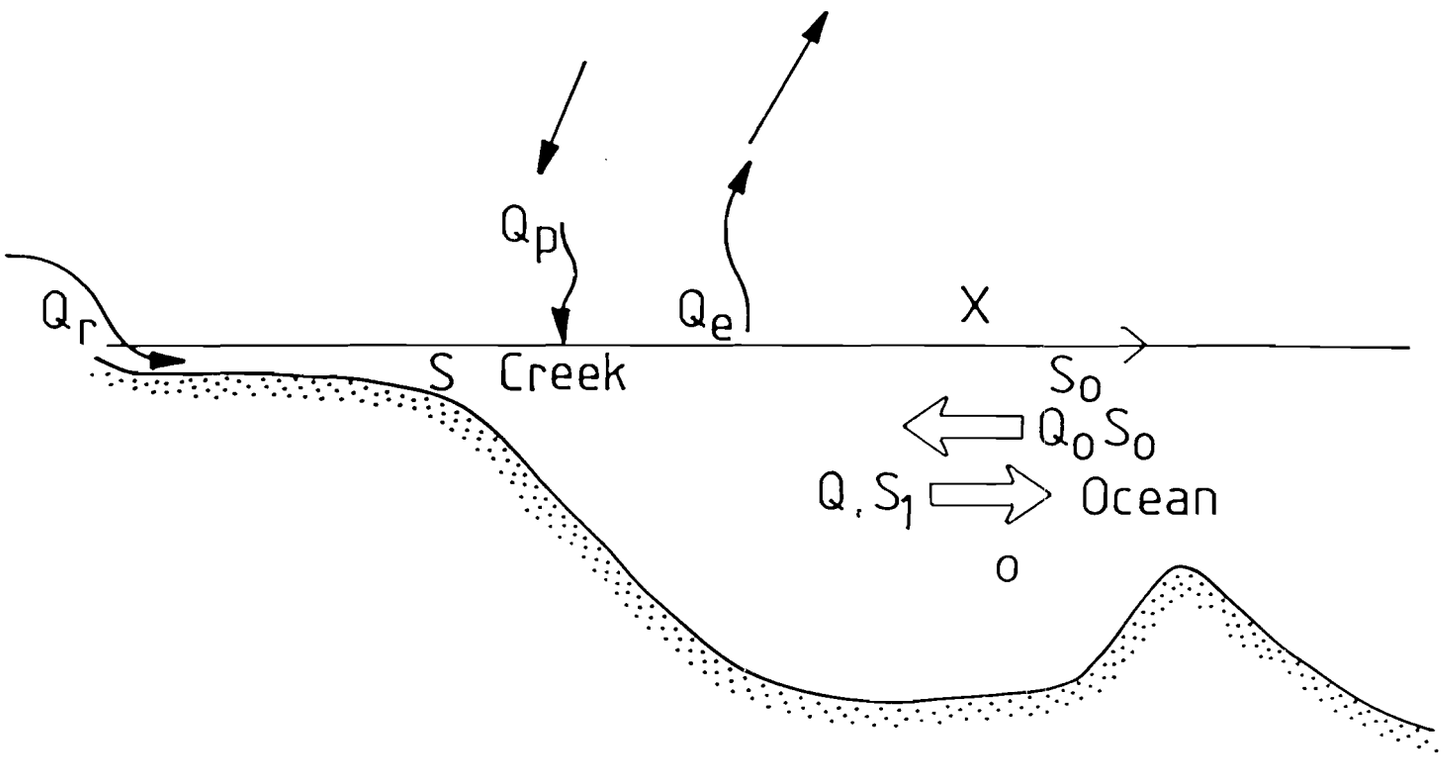

Figure 12.

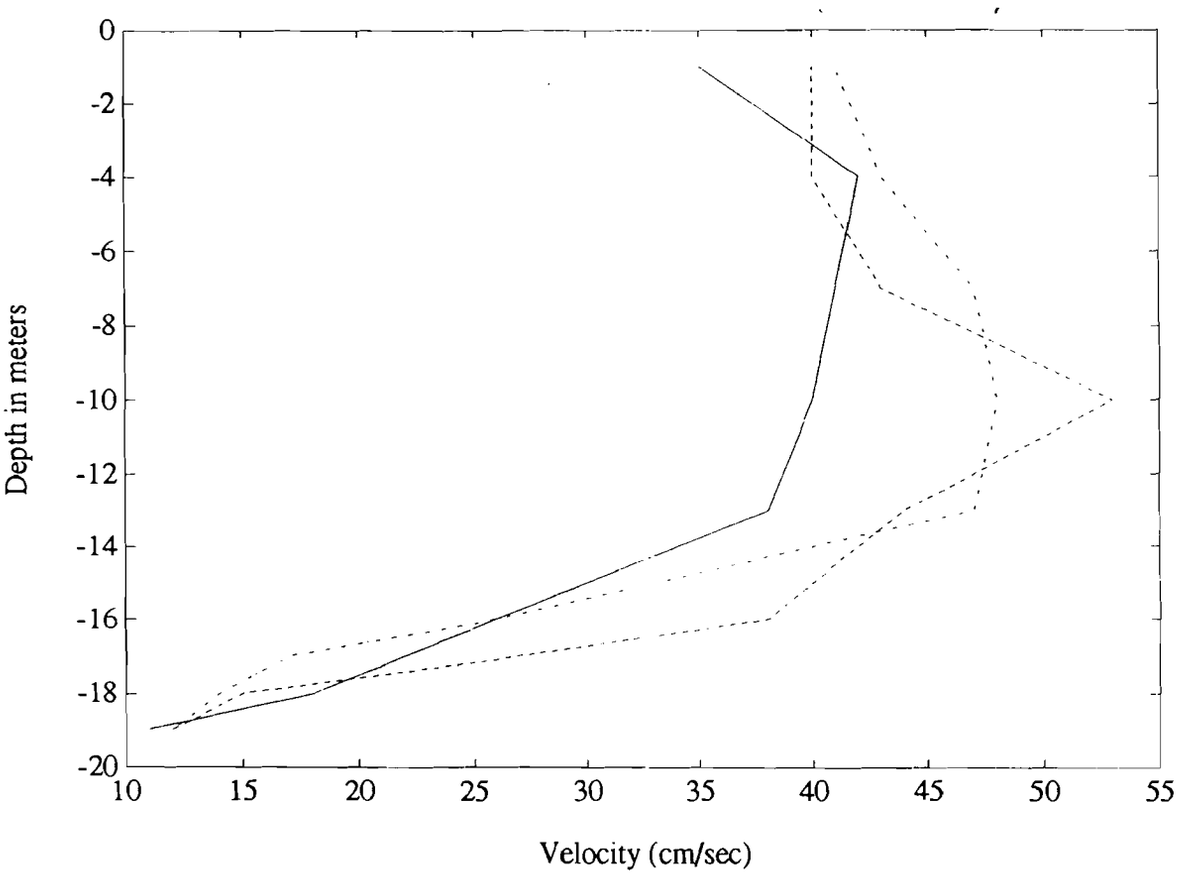
0
-2
-4
-6
-8
-10
-12
-14
-16
-18
-20
10
15
20
25
30
35
40
45
50
55
Depth in meters
Velocity (cm/sec)